Design, synthesis, structure-activity relationship studies, and three-dimensional quantitative structure-activity relationship (3D-QSAR) modeling of a series of O-biphenyl carbamates as dual modulators of dopamine D3 receptor and fatty acid amide hydrolase

Alessio De Simone,[1†] Debora Russo,[2] Gian Filippo Ruda,[2†] Alessandra Micoli,[1†] Mariarosaria Ferraro,[1] Rita Maria Concetta Di Martino,[1] Giuliana Ottonello,[2] Maria Summa,[2] Andrea Armirotti,[2] Tiziano Bandiera,[2] Andrea Cavalli,[1,3] Giovanni Bottegoni.[1,4]*

[1] CompuNet, Istituto Italiano di Tecnologia, 16163 Genova (GE), Italy; [2] PharmaChemistry, Istituto Italiano di Tecnologia, 16163 Genova (GE), Italy; [3] FaBit, Università di Bologna, 40127 Bologna (BO), Italy; [4] BiKi Technologies, Genova (GE), Italy.

ABSTRACT

We recently reported molecules designed according to the multi-target-directed ligand paradigm to exert combined activity at human fatty acid amide hydrolase (FAAH) and dopamine receptor subtype D3 (D3R). Both targets are relevant for tackling several types of addiction (most notably nicotine addiction) and other compulsive behaviors. Here, we report an SAR exploration of a series of biphenyl-N-[4-[4-(2,3-substituted-phenyl)piperazine-1-yl]alkyl]carbamates, a novel class of molecules that had shown promising activities at the FAAH – D3R target combination in preliminary studies. We have rationalized the structural features conducive to activities at the main targets, and investigated activities at two off-targets: dopamine receptor subtype D2 and endocannabinoid receptor CB_1. To understand the unexpected affinity for the CB_1 receptor, we devised a 3D-QSAR model, which we then prospectively validated. Compound **33** was selected for PK studies because it displayed balanced affinities for the main targets and clear selectivity over the two off-targets. **33** has good stability and oral bioavailability, and can cross the blood-brain barrier.

INTRODUCTION

Multi-target-directed ligands (MTDLs) are small organic molecules purposely designed to interact with multiple biological targets.[1] Developed within the framework of polypharmacology, the basic concept behind this relatively novel but already consolidated approach is quite simple: when a single molecule modulates multiple selected targets, it can have synergistic efficacy, milder side-effects, and a lower probability of triggering resistance or drug-drug interactions. MTDLs may thus overcome the limitations of the traditional "one drug, one target" approach.[2-3] MTDLs can be seen as a straightforward way to put into practice the insights of network medicine, which approaches the etiology and, possibly, the treatment of diseases as perturbations of complex and interconnected signaling pathways.[4] Thus, research on MTDLs has traditionally focused on treating complex and multifaceted conditions such as neurodegeneration,[5-6] cancer,[7-8] and infectious diseases.[9]

We recently began investigating the possibility of developing MTDLs to treat tobacco addiction. Responsible for over five million deaths every year, tobacco smoking is the single most common cause of avoidable death in Western countries.[10] Tobacco contains harmful chemicals that are directly connected to about 33% of all cancer deaths, including about 90% of all cases of lung cancer, the most deadly form of cancer.[11] However, the actual addiction to tobacco is caused by the alkaloid nicotine.[12-13] Nicotine elevates the dopaminergic tone in specific areas of the brain, including the ventral tegmental area (VTA) and the nucleus accumbens (NAc). These areas belong to the mesocorticolimbic system, a brain circuit that is critical in natural and drug-induced reward and motivated behavior. This is nicotine's best understood effect, and it is mediated by interaction with nicotinic acetylcholine receptors (nAChRs) in the brain.

Nicotine's effects have also been associated with alterations in most of the main neurotransmitter systems, including biogenic amines, amino acid transmitters such as glutamate and gamma-aminobutyric acid (GABA), opioids, and endocannabinoids.[14] For example, the activity of dopamine neurons in the VTA is regulated by nAChR-expressing glutamatergic and GABAergic neurons. In this circuit, the balance between the stimulating and repressing actions of the two neurotransmitters is crucial for modulating dopamine levels in the NAc. Moreover, presynaptic CB_1 receptors located on GABAergic fibers or on glutamatergic interneurons have been shown to abolish GABA-dependent tonic inhibition of dopamine neurons, facilitating nicotine actions.[15-16] This profound and widespread modification of multiple neurotransmitter levels is conducive to a complex behavioral condition dominated by withdrawal symptoms, craving, drug-seeking, and reinforcing effects. This complexity may explain why none of the currently proposed pharmacological treatments for nicotine addiction have long-lasting efficacy.[17] Varenicline, a nicotine receptor partial agonist, and Bupropion, a norepinephrine-dopamine reuptake inhibitor and nicotine receptor antagonist, are marketed drugs for the treatment of nicotine addiction.[18] These molecules have shown promising results in counteracting nicotine cravings and withdrawal symptoms. However, as mentioned, their effectiveness in promoting long-term abstinence avoiding relapse is quite limited. Furthermore, their mechanism of action, based on directly interfering with the cholinergic transmission in various brain areas connected to reward and gratification, is likely responsible for the mild to intense severity of the side effects (e.g., eating disorders, suicidal thoughts) associated with treatments based on these molecules.[19] For these reasons, nicotine addiction remains a largely unmet medical need. Hence, our idea of tackling nicotine addiction by means of MTDLs that can concurrently modulate the dopamine receptor subtype D3 (D3R) and the human fatty acid amide hydrolase (FAAHFAAH), likely

eliciting enduring effectsFAAHFAAH. D3R is a G-protein-coupled receptor that is predominantly expressed in the mesocorticolimbic system. For many years, D3R has been the focus of synthetic chemistry campaigns to develop drugs to treat addiction and compulsive behaviors.[20-21] Specific overexpression of D3R has been observed in nicotine-exposed brains and is a common feature of drug addictions.[22] Earlier studies focused on developing antagonists, while more recent investigations have sought to develop potent and selective partial agonists.[23] Pharmacologically, partial agonists are more appealing because they provide a functional response, which depends on dopamine levels in the mesolimbic area. In the absence of dopamine (after withdrawal), a partial agonist would act as a functional agonist with lower intrinsic efficacy. In the presence of the natural substrate, it would functionally antagonize dopamine binding to D3R, preventing the reinstatement of nicotine-induced signaling circuits. In contrast, pure D3R antagonists are of limited use in alleviating withdrawal symptoms, but they are more effective in reducing craving, drug-seeking, relapse, and reinforcement effects.[24-25] FAAH inhibition has only recently been considered as a potential strategy for treating addiction.[26] FAAH's physiological role is to terminate the endocannabinoid (EC) signaling by cleaving anandamide (AEA), one of the agonists of the endogenous CB_1 receptor (CB_1 R).[27] Interestingly, while considerable evidence has emerged that directly links the endocannabinoid system to nicotine addiction, FAAH's role is likely to be mediated by non-cannabinoid signaling pathways.[28] FAAH is also responsible for cleaving two more substrates: oleoylethanolamide (OEA) and palmitoylethanolamide (PEA), which are endogenous agonists of the nuclear receptor PPAR-α. Activating PPAR-α stimulates the activation of tyrosine kinases, which in turn leads to the phosphorylation and negative regulation of neuronal nAChR. Inhibiting FAAH in order to maintain artificially high levels of OEA and PEA thus appears to be a reasonable strategy for

pharmacologically counteracting the effects of nicotine.[29] Furthermore, region-specific FAAH inhibition leads to increased levels of EC, with the potential of modulating in a more effective way nicotine-related behaviors as compared to effects observed after ubiquitous activation of CB_1Rs by direct agonists, suggesting that selective alterations of FAAH activity in limbic regions of the brain could have a key role in the development of addictive behaviors.[26] Increased AEA levels due to FAAH inhibition can likely activate CB_1 receptors on glutamatergic neurons that, in turn, negatively modulate dopamine release in NAc, interfering with the creation of the addiction cycle. Last, the activation of CB_1R has been associated to anxiolytic effects, which can be useful in the treatment of negative emotional states during withdrawal.[30] Inhibition by FAAH inhibitor URB597 was recently reported to prevent self-administration and cue- and substance-induced reinstatement in animal models of nicotine addiction.[26] In 2014, we reported the first set of rationally designed compounds endowed with potent in vitro activities against these two targets. Our compounds turned out to be potent FAAH inhibitors and D3R partial agonists.[31-32] While the *O*-naphthyl carbamate series of compounds, exemplified by **1** (see Figure 1), was fairly selective with respect to the investigated off-targets, the biphenyl-bearing molecules **2** and **3** displayed unexpected and potent activity at CB_1 R (EC_{50} 0.3 nM and 0.9 nM, respectively). Here, we report on an extensive SAR exploration of a series of biphenyl-N-[4-[4-(2,3-substituted- phenyl)piperazine-1-yl]alkyl]carbamates, which helped identify the structural drivers for the desired activities at the two targets. This study also helped rationalize activities at the investigated off-targets, pointing to potential strategies for designing more selective compounds.

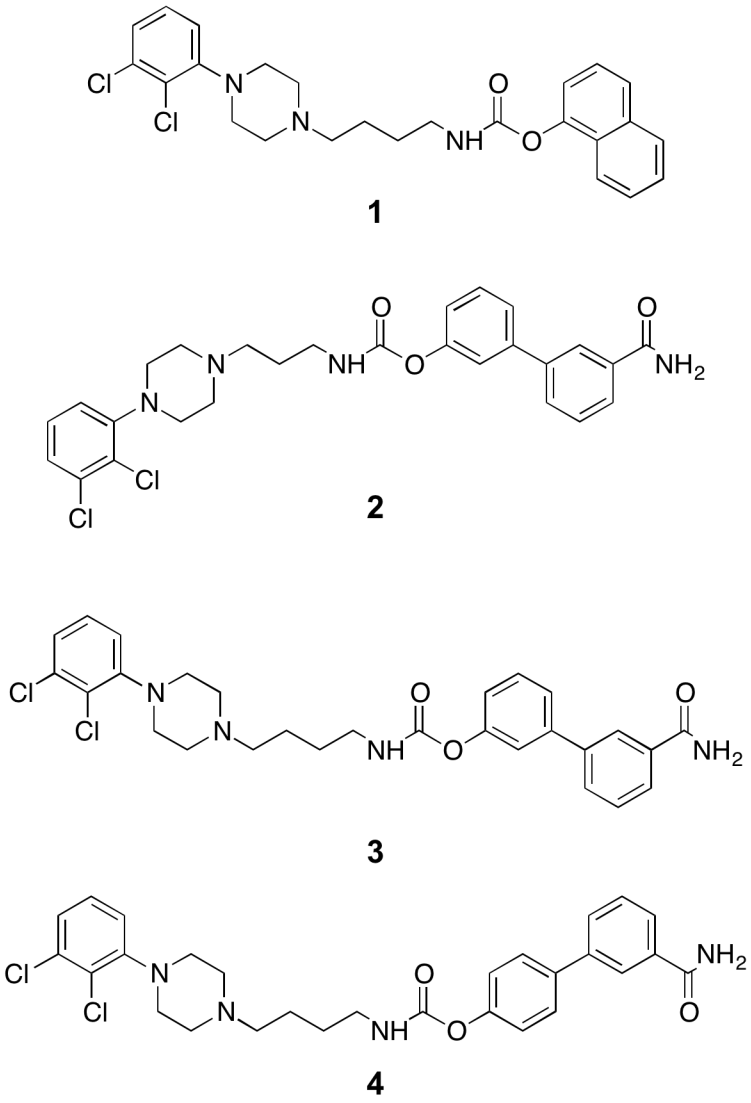

Figure 1. Previously reported O-biphenyl carbamates with dual D3R and FAAH activity

CHEMISTRY

The syntheses of the compounds are largely based on well-described reactions. Scheme 1 reports the synthetic pathway used to prepare the final carbamate derivatives. Amines with general structure **7** were obtained by alkylation of arylpiperazine derivatives **5** with different commercially available bromoalkylphthalimides **6** (Scheme 1, see Supporting Information for details). The obtained phthalimides were deprotected by treatment with hydrazine. In the final

step, the obtained amines were activated as isocyanates by reaction with a slight excess of Boc anhydride and 4-dimethylamino pyridine (DMAP) in acetonitrile. These were then reacted with the appropriate phenol derivatives to produce the various final carbamates. An alternative procedure involved activating the amine derivative with *p*-nitrophenylchloroformate and then reacting with the phenolic derivatives.

Scheme 1. Synthetic route to compounds 16-29, 32-37, and 40-42

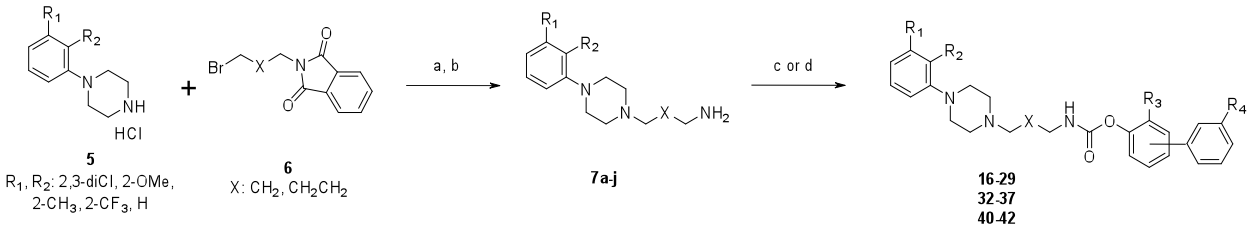

Reagents and conditions: a) CH_3CN, K_2CO_3, reflux, 6 h. Yields: 83-99%; b) Hydrazine monohydrate, MeOH, 80 °C, 2 h, then 2N HCl, 1 h. Yields: 53-88%; c) ArOH, $(Boc)_2O$, DMAP, CH_3CN, rt, 23 h. Yields: 7-50% d) ArOH, *p*-nitrophenylchloroformate, DIPEA, DMA:DCM 1:1, rt, overnight. Yields: 10-26%.

For the synthesis of the non-commercially available phenolic derivatives, different procedures were applied and are outlined in Scheme 2. Biphenyl alcohols of general formula **10** were prepared with a modified Suzuki cross-coupling reaction[33] between commercially available aryl halides and boronic acid derivatives **8** and **9**, in the presence of a catalytic amount of palladium acetate in a medium of water and ethylene glycol monomethyl ether (EGME). This procedure provided the desired products in high yield and with good reproducibility. When R_3 is a methoxy group, this procedure is ineffective for the steric hindrance of this group on the

halogen atom. In these attempts, $PdCl_2$(dppf) was used as a catalyst (Scheme 2, see Supporting Information for details).

Scheme 2. Preparation of noncommercially available phenolic derivatives

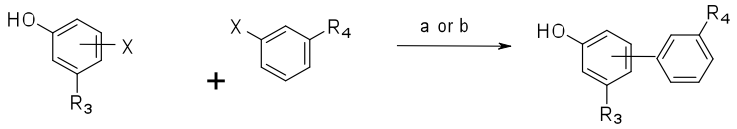

8
X= Br, $B(OH)_2$
R_3= H, F, OMe

9
X= Br, $B(OH)_2$
R_4= H, $CONH_2$

10a-h

Reagents and conditions: a) $Pd(OAc)_2$, K_2CO_3, EGME/H_2O, rt, 5 min Yields: 58-97%. b) $PdCl_2$(dppf), K_2CO_3, 1,4-Dioxane: Water 3:1, 90 °C, 3 hours. Yield: 48% (average of two attempts).

To synthesize analogues bearing an alkene in the linker (**30-31**), the synthesis started from trans-1,4-dichloroalkene **12** and potassium phthalimide **11** to yield intermediate **13** (Scheme 3). Then, reaction with arylpiperazine **5** and deprotection with hydrazine afforded the desired amine **15** in good yields. The amine was used in a reaction with biphenolic derivatives **10b-c** (prepared using the same conditions reported in Scheme 2) in the presence of Boc_2O and DMAP to obtain the carbamate derivative **30-31**, as shown in Scheme 3.

Scheme 3. **Synthetic route to alkenyl derivatives 30 and 31**

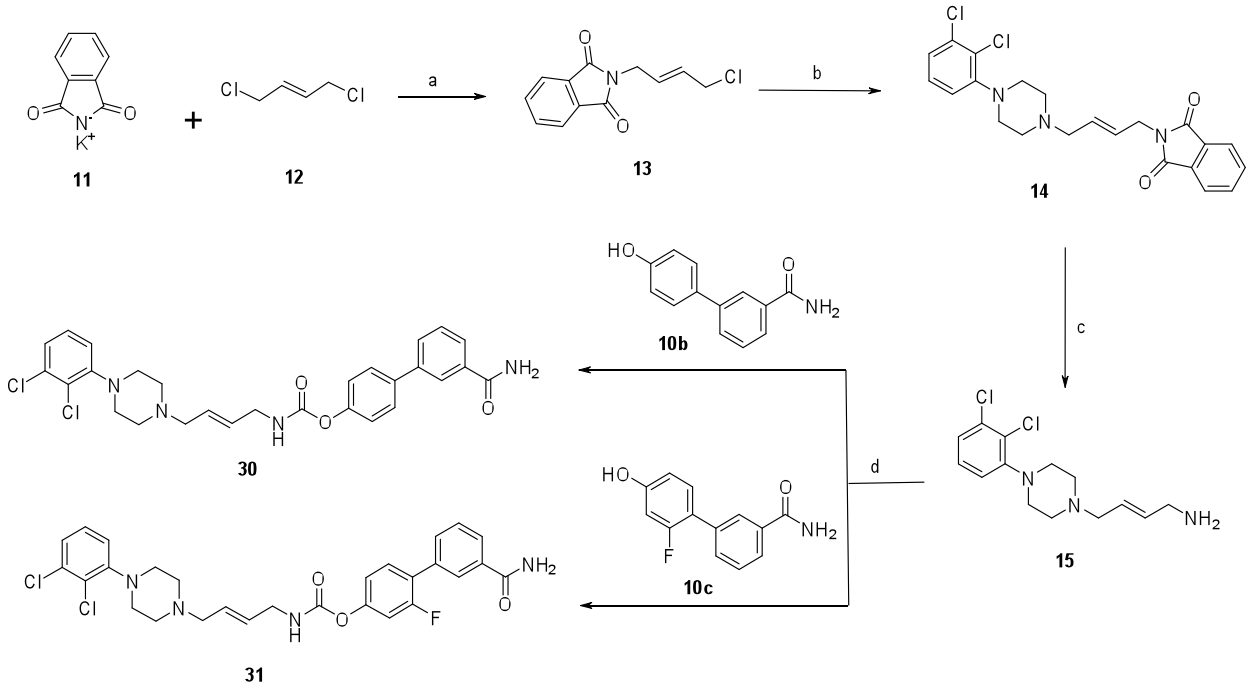

Reagents and conditions: a) DMF, rt, under nitrogen atmosphere, overnight. Yield: 67%. b) 1-(2,3-dichlorophenyl)piperazine, K_2CO_3, MeCN, reflux, 6 hours. Yield: 83%. c) $NH_2NH_2 \cdot H_2O$, MeOH, then 2N HCl, reflux, 3 hours. Yield: 88%. d) Boc_2O, DMAP, MeCN, rt, 20-25 hours. Yields: **30**: 16%; **31**: 22%.

RESULTS AND DISCUSSION

The newly synthesized compounds fit into the general structure reported in Figure 2.

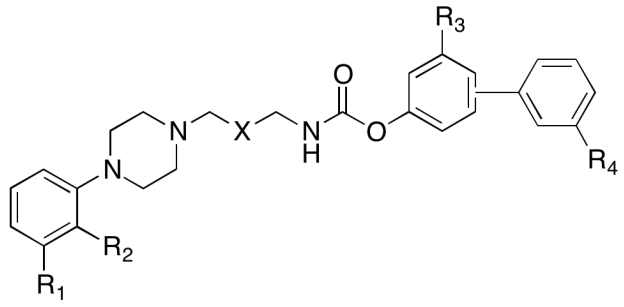

Figure 2. General structure of the newly synthesized dual D3R FAAH modulators

We sought to characterize the SAR for this class of compounds by introducing different substituents on the aromatic ring of the aryl-piperazine and investigating both *meta* (*m*-) biphenyl-bearing and *para* (*p*-) biphenyl-bearing compounds. We also considered the role of the carboxamide in the distal ring of the *O*-biphenyl moiety. Finally, we studied a limited set of variants by exploring substituents of the proximal ring in the biphenyl group as well as the role of the alkyl spacer. We evaluated the biological activities of the reported compounds as FAAHFAAH inhibitors and D3R modulators by means of a fluorescent assay and a cellular functional assay, respectively. To manage our resources, we only assessed compounds for selectivity for D2R and CB_1R if they were also characterized by reasonable activities at the main targets (FAAHFAAH IC_{50} < 60 nM, D3R EC_{50} < 100 nM, and no more than two orders of magnitude less potent than **4**; D3R efficacy < 75% as compared to 300 nM dopamine, as we were interested in developing D3R partial agonists). Considering our starting point in the biphenyl series, we sought an initial selectivity ratio with respect to the investigated off-targets of at least one order of magnitude. The results are reported in Table 1.

Table 1. Results of the SAR studies.

Structure

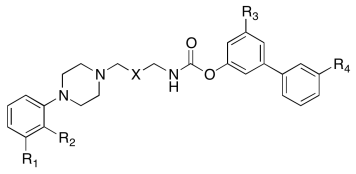

Compound	R_1	R_2	X	R_3	R_4	HCl salt	Human FAAH IC_{50} (nM)[a]	D3R EC_{50} (nM)	D3R % Efficacy[b]	D2R EC_{50} (nM)	D2R% Efficacy[b]	CB_1 EC_{50} (nM)
2 [c]	Cl	Cl	CH_2	H	$CONH_2$	no	0.6	1.0	56	13.0	22	14.0
3 [c]	Cl	Cl	CH_2 CH_2	H	$CONH_2$	no	1.6	6.5	52	45	39	0.9
16	H	OMe	CH_2	H	$CONH_2$	no	1.8±0.4	19.0	60	54.2	46	1.4
17	H	OMe	CH_2CH_2	H	$CONH_2$	no	2.3±0.3	14.0	34	56.4	92	2.3
18	H	H	CH_2	H	$CONH_2$	no	1.3±0.1	2.1	>90			
19	H	H	CH_2CH_2	H	$CONH_2$	no	1.1±0.2	3.7	77			
20	Cl	Cl	CH_2CH_2	H	H	yes	4.1±0.7	240.0	>90			

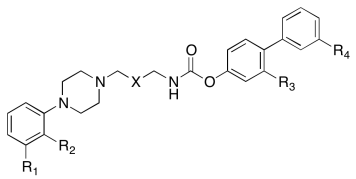

4 [c]	Cl	Cl	CH_2 CH_2	H	$CONH_2$	no	0.6	1.0	56	13.0	22	14.0
21	Cl	Cl	CH_2	H	$CONH_2$	no	0.5±0.2	0.9	77	39.9	56	6.1
22	H	OMe	CH_2	H	$CONH_2$	no	2.8±0.3	7.4	64	21.5	46	2.6
23	H	OMe	CH_2CH_2	H	$CONH_2$	yes	10.7±1.2	0.9	57	53.0	48	320
24	H	Me	CH_2CH_2	H	$CONH_2$	no	3.0±0.6	4.0	74	49.3	18	52
25	H	CF_3	CH_2CH_2	H	$CONH_2$	no	2.7±0.4	11.0	69			
26	H	H	CH_2CH_2	H	$CONH_2$	no	3.5±0.4	3.6	88			
27	Cl	Cl	CH_2CH_2	F	$CONH_2$	no	1.0±0.2	18.6	74	13.7	40.4	15
28	Cl	Cl	CH_2CH_2	OMe	$CONH_2$	no	2.7±0.1	4.4	83			
29	H	OMe	CH_2CH_2	OMe	$CONH_2$	no	63.0±20.0	3.9	52	10.4	66	110
30	Cl	Cl	CHCH	H	$CONH_2$	no	1.2±0.1	37.8	A [d]	147.0	22	20
31	Cl	Cl	CHCH	F	$CONH_2$	no	0.6±0.2	6.9	A [d]	66.2	51	9.2
32	Cl	Cl	CH_2	H	H	no	3.3±0.6	17.0	43	14.7	65	70
33	Cl	Cl	CH_2CH_2	H	H	yes	0.9±0.1	18.0	65	135.0	48	1500
34	H	OMe	CH_2	H	H	yes	2.6±0.5	14.0	82			
35	H	OMe	CH_2CH_2	H	H	yes	39±7.4	330.0	85			
36	H	Me	CH_2CH_2	H	H	no	7.6±1.5	130.0	>90			
37	H	CF_3	CH_2CH_2	H	H	no	20.7±7.4	1200.0	>90			

[a] n=3; [b] as of 300 nM of dopamine; [c] activity (FAAHFAAH, D3R, CB_1) and efficacy (D3R) data as reported in reference 28; [d] Antagonist.

SAR Studies. We further investigated the properties of the *m*-biphenyl series by introducing the classic 2-methoxy substituent in the aryl-piperazine in the presence of three- (**16**) and four-methylene-unit (**17**) linkers.[20] With respect to **2** and **3**, their 2,3-di-Cl-substituted counterparts, both derivatives maintained potent activities at the main targets (Table 1), with the 2-methoxy substituent being only slightly detrimental for D3R activity. In line with results reported for **2**

and **3**, **16** and **17** were also potent CB_1R agonists with 1.4 nM and 2.3 nM EC_{50} values, respectively. Derivatives **18** and **19**, displaying a naked pendant aromatic ring, maintained potent and balanced activities at both targets, but their D3R activation profile switched significantly toward a full agonist effect. Eliminating the carboxamide in the distal *m*-biphenyl ring in **20** severely reduced the activity against D3R.

The results for **4** suggested that a potent dual modulator profile devoid of selectivity problems could be achieved by introducing a *p*-biphenyl group at the *O*-side of the carbamate. We therefore turned our attention to derivatives bearing this moiety. Reducing the length of the linker of **4** to three methylene units (**21**) was not detrimental for activities at the main targets (Table 1). However, while over 50-fold selectivity over D2R could be obtained, **21** displayed 6.1 nM EC_{50} at CB_1R. Studying the effect of substituents in the aromatic ring of the aryl-piperazine, we observed that, when we introduced a 2-methoxy group in combination with a three-methylene-unit linker, compound **22** maintained potent activities at FAAH and D3R but did not achieve selectivity toward both the off-targets. When the same substitution was coupled with a longer linker (**23**), activity at D3R was maintained and activity at FAAH was only slightly affected. Notably, activity at CB_1R decreased by up to 320 nM. Introducing smaller substituents at position 2, as with the 2-methyl-bearing (**24**) and 2-trifluoromethyl-bearing (**25**) derivatives, did not affect activity at the two targets but did lead to increased efficacy at D3R, shifting activity closer to a full agonist profile. Compound **24** had moderate 18-fold selectivity toward D2R and acceptable selectivity with respect to CB_1R (4.0 nM EC_{50} at D3R and 52 nM EC_{50} at CB_1R). Consistently, and in line with the results obtained with the *m*-biphenyl derivatives, compound **26**, bearing a naked phenyl ring, behaved almost like a full agonist (88% efficacy).

We also introduced some substituents in the proximal ring of the biphenyl moiety. To address possible solubility issues, we introduced a fluorine atom, which endowed **27** with sub-nanomolar inhibitory potency against FAAH. However, activity at D3R (18 nM EC_{50}) was almost 20 times less than that observed for **4**. Most importantly, this derivative displayed no selectivity with respect to the off-targets. As previously reported by Moreno-Sanz and coworkers, a methoxyl group introduced in the proximal ring of the biphenyl should further improve inhibitory potency at FAAH without compromising brain penetration.[34] Indeed, **28** turned out to be a potent FAAH inhibitor (2.7 nM IC_{50}) but its efficacy at D3R shifted toward pure agonism. Conversely, when this substitution was coupled with a 2-methoxyl substituent in the aryl-piperazine (**29**), the partial D3R agonist profile was restored but inhibitory activity at FAAH decreased quite substantially (63 nM IC_{50}). Introducing an unsaturation in the linker (**30**) decreased activity at D3R (EC_{50} 37.8 nM) while maintaining activity at FAAH (IC_{50} 1.2 nM). Introducing a fluorine group in the proximal biphenyl ring (**31**) restored activity at D3R in the single digit nanomolar range. Interestingly, **30** and **31** behaved as D3R antagonists. As expected in light of classic studies of D3R modulators,[35] the presence of a central trans double-bond in the linker lowered the affinity for D2R, which decreased with respect to the saturated analogues from 23 nM (**4**) to 147 nM (**30**) and from 13.7 nM (**27**) to 66.2 nM (**31**). However, neither **30** nor **31**, with EC_{50} values of 20 nM and 9.2 nM, respectively, displayed selectivity toward CB_1R.

To assess the effects of the carboxamide in the distal ring of the biphenyl region, we synthesized and tested several compounds lacking this substituent. Activity data are reported in Table 1 and systematically compared to those of the carboxamide-bearing analogues. 2,3-di-Cl-substituted aryl-piperazine compounds **32** and **33** were characterized by potent activities at FAAH in line with those of **21** and **4**. In **32**, activity at D3R decreased with respect to **21** (see

Table 1); consistently, in **33**, D3R EC_{50} increased from 1.0 nM to 18 nM. In terms of selectivity, an acceptable ratio could be achieved for D2R. Remarkably, activity at CB_1R dropped substantially in **32** (EC_{50} 70 nM) with respect to **21** and decreased in **33** by over two orders of magnitude (EC_{50} 1500 nM) with respect to **4**. The 2-methoxy substituted compound **34** preserved potent and balanced activities at both main targets, but its efficacy shifted toward an agonist profile (D3R efficacy 82%). In the four-methylene-unit linker analog **35**, activities decreased at both targets, with FAAH IC_{50} equal to 39 nM and D3R EC_{50} to 330 nM (efficacy 85%). In agreement with the behavior of **35**, introducing a 2-methyl- (**36**) or a 2-trifluoromethyl- (**37**) group in the pendant aromatic ring of the carboxamide-lacking derivatives led to a significant drop in D3R activity (Table 1).

In light of these results, we propose a first rationale for the chemical features required for a balanced and potent activity at FAAH and D3R. Substitutions on the pendant aromatic ring of the aryl-piperazine were required for a partial agonist profile against D3R. In the presence of a saturated linker, bulkier substituents shifted the efficacy profile toward antagonism. Regarding the linker, the four-methylene-unit linker resulted in lower activation of D3R than the three-methylene-unit linker, and was thus preferred in order to have partial agonist derivatives. By introducing a central trans double-bond to increase the system's rigidity, we obtained D3R antagonists. These results are in qualitative agreement with previous studies by Newman and colleagues on how substitutions at the terminal aromatic ring, in combination with different linkers, can affect efficacy.[36] Regarding FAAH, a longer linker, especially when combined with a bulkier substituent in position 2, led to a drop in activity. This may be due to a more constrained fit in the binding pocket region known as the acyl chain binding channel. At the *O*-side of the carbamate, the distal phenyl ring could be placed in both the *m*- and *p*-positions of the proximal

ring without affecting the potencies against the two main targets. For the *p*-biphenyl derivatives, a substituent in the *meta* position of the proximal phenyl ring could be inserted without dramatically altering activities. The carboxamide substituent on the distal ring revealed a beneficial role in the affinity for D3R, possibly because of an H-bond interaction with Thr92, which was consistently suggested by our previous docking experiments.[31] However, while consistent across the series, the loss in D3R affinity due to the deletion of the carboxamide was less severe for compounds with the 2,3-di-Cl-substitution in the arylpiperazine. In FAAH, the activity of our derivatives was only marginally affected by the presence of the carboxamide, although the reported activities of known inhibitors URB524 (naked biphenyl group in the *O*-side of the carbamate, FAAH IC_{50} 63 nM)[37] and URB597 (carboxamide substituted biphenyl ring, FAAH IC_{50} 4.6 nM)[38] had suggested this would not be the case. This was probably due to the presence of an elongated substituent at the N-side of the carbamate, which is here the key structural driver for the FAAH inhibitory effect.[39] These SAR considerations are summarized in Figure 3.

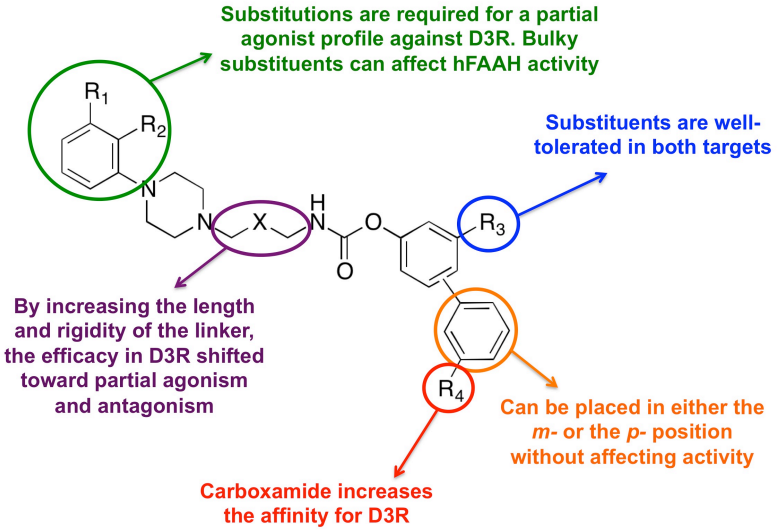

Figure 3. Summary of the results of SAR studies performed on different regions of the synthesized derivatives.

Selectivity at the off-targets. Twelve derivatives that showed a promising activity profile for the main targets were assessed for selectivity for D2R and CB_1R. For D2R, some general considerations can be outlined. With the sole exception of **27**, in which affinities for D3R and D2R were almost equivalent, our compounds had greater affinity for D3R than for D2R. This is not surprising, given that the original concept for these compounds was to introduce a carbamate as a conservative variation of a classic D3R-selective pharmacophore.[20] The aryl carbamate protrudes outside the orthosteric binding site in a region defined by the extracellular loop 3 and transmembrane helices I, II, and VII (secondary binding site). Selectivity can be obtained by exploiting subtle differences in both side chain and backbone rearrangements in this region.[40] Selectivity over D2R decreased: i) in *p*-biphenyl derivatives with respect to their *m*-biphenyl counterparts, ii) in molecules bearing a shorter linker, and iii) in 2-methoxy substituted molecules (Table 1). Again, this is consistent with previously reported studies indicating that selectivity for D3R over D2R is affected by the nature and (most importantly) orientation of the portion of the molecule in contact with the secondary binding site.[36] In turn, this orientation varies in the two receptor subtypes depending on the substituents in the aryl-piperazine and the linker length. While the present study did not match the remarkable D2R/D3R selectivity ratio that characterized our previously described derivatives **2** and **3**, as well as classic arylamide-based D3R modulators reported in the literature,[41] several compounds obtained did display sufficient selectivity.

From a structural perspective, the CB_1R activity data was more puzzling. A three-unit linker usually led to increased activity at CB_1R so long as it was coupled to the carboxamide substituent

in the distal phenyl ring. The presence of this substituent was the structural feature exerting the more evident effect, as suggested by activity data on **32** and **33** (Table 1). We hypothesized that these results could be interpreted within the framework of the classic SAR of CB_1R agonists.[42] Figure 4 reports the structures of four prototypical CB_1R agonists, namely Δ^9-THC (**38**, CB_1R EC_{50} 10.2 nM), HU-210 (**39**, CB_1R EC_{50} 0.73 nM), JWH-051 (**40**, CB_1R EC_{50} 1.2 nM), and JWH-133 (**41**, CB_1R EC_{50} 667 nM).

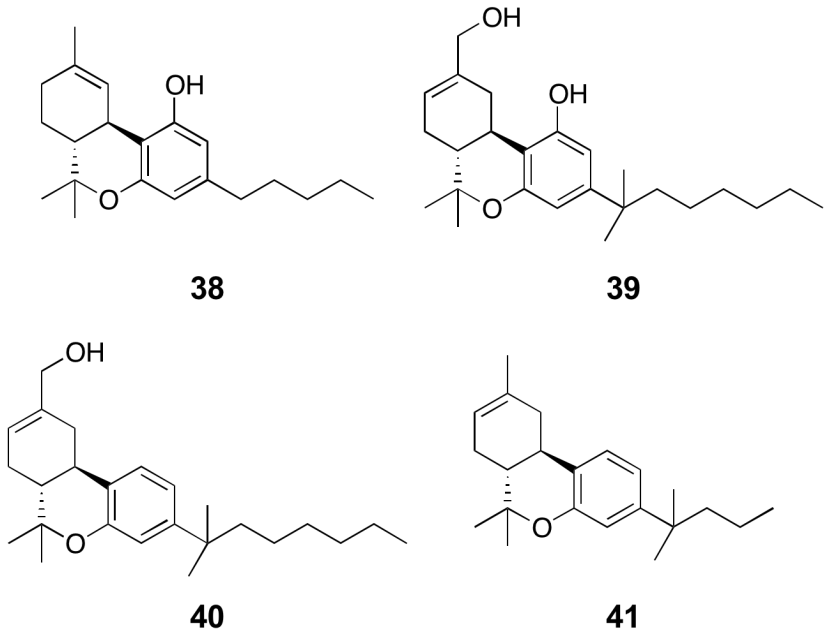

Figure 4. Structures of four CB_1R agonists

No crystal structure of an agonist-bound CB_1R was available when we conducted our study; however, several reports have suggested that the aliphatic chain of classic CB_1R agonists lays perpendicular to the plane of the tricyclic system.[43-44] This is also consistent with the pose adopted by Δ^9-THC docking studies carried out at the recently reported crystal structure of antagonist-bound CB_1R.[45] Using as a template a conformation of the sub-nanomolar agonist **39** that reflected this arrangement, we performed an APF-based structural alignment (see

Experimental Section) and generated an overlapping conformation of **4** (Figure 5A).[46] The resulting structural alignment, with the biphenyl group matching the tricyclic system, is particularly evocative, as the classic SAR of THC analogs could be applied to our molecules. First, the presence of a hydroxyl group in position 1 (**38**) is very important for eliciting potent activity. Another hydrogen bond donor/acceptor group in position 11 can further increase activity (**39**) or can maintain activity if the hydroxyl group in 1 is removed (**40**). The removal of both hydrogen bond donor groups is detrimental for activity, as exemplified by **41**. This would explain the strong effect of the carboxamide substituent. Second, the aliphatic chain of CB_1R agonists can be modified quite substantially without compromising activity, even if elongated or decorated with bulky pendants. Hence, it stands to reason that linker and aryl-piperazine could be lodged in the corresponding region without compromising activity. Finally, it has been reported that CB_1R activity is modulated by the planarity of the tricyclic system, with more planar systems being less active and more susceptible to the effect of the substitutions in positions 1 and 11, respectively. To further test the hypothesis that CB_1R activity can be explained by the classic SAR of THC analogs, we synthesized three novel compounds (**42**-**44**), introducing a flat aromatic group at the *O*-side of the carbamate. Potent and selective D3R modulators displaying rigid tricyclic systems have already been reported.[47]

Table 2. Activity data of the carbazole-based analogs

Compound	Structure	Human FAAH IC_{50} (nM)[a]	D3R EC_{50} (nM)	D3R% Efficacy[b]	D2R EC_{50} (nM)

									CB$_1$
								D2R%	EC$_{50}$
	R$_1$	R$_2$	X					Efficacy[b]	(nM)
42 (15197)	Cl	Cl	CH_2	4.8±2.0	150.0	>90			380
43 (15387)	Cl	Cl	CH_2CH_2	8.0±0.8	120.0	>90			370
44 (15959)	H	OMe	CH_2CH_2	37.0±10.0	12.0	66	57.9±18.8	44	2300

[a] n=3; [b] as of 300 nM of dopamine;

As expected, CB$_1$R activity was significantly reduced in all three derivatives: **42**, EC$_{50}$ 380 nM; **43**, EC$_{50}$ 370 nM; and **44**, EC$_{50}$ 2300 nM. However, **42** and **43** displayed reduced activity at D3R (D3R EC$_{50}$ 150 nM and 120 nM, respectively), and **44** coupled an only mild selectivity over D2R (D2R/D3R selectivity ratio equal 4.8) with a reduced activity against FAAH (FAAH IC$_{50}$ 37 nM). Therefore, we did not investigate further carbazole-bearing derivatives.

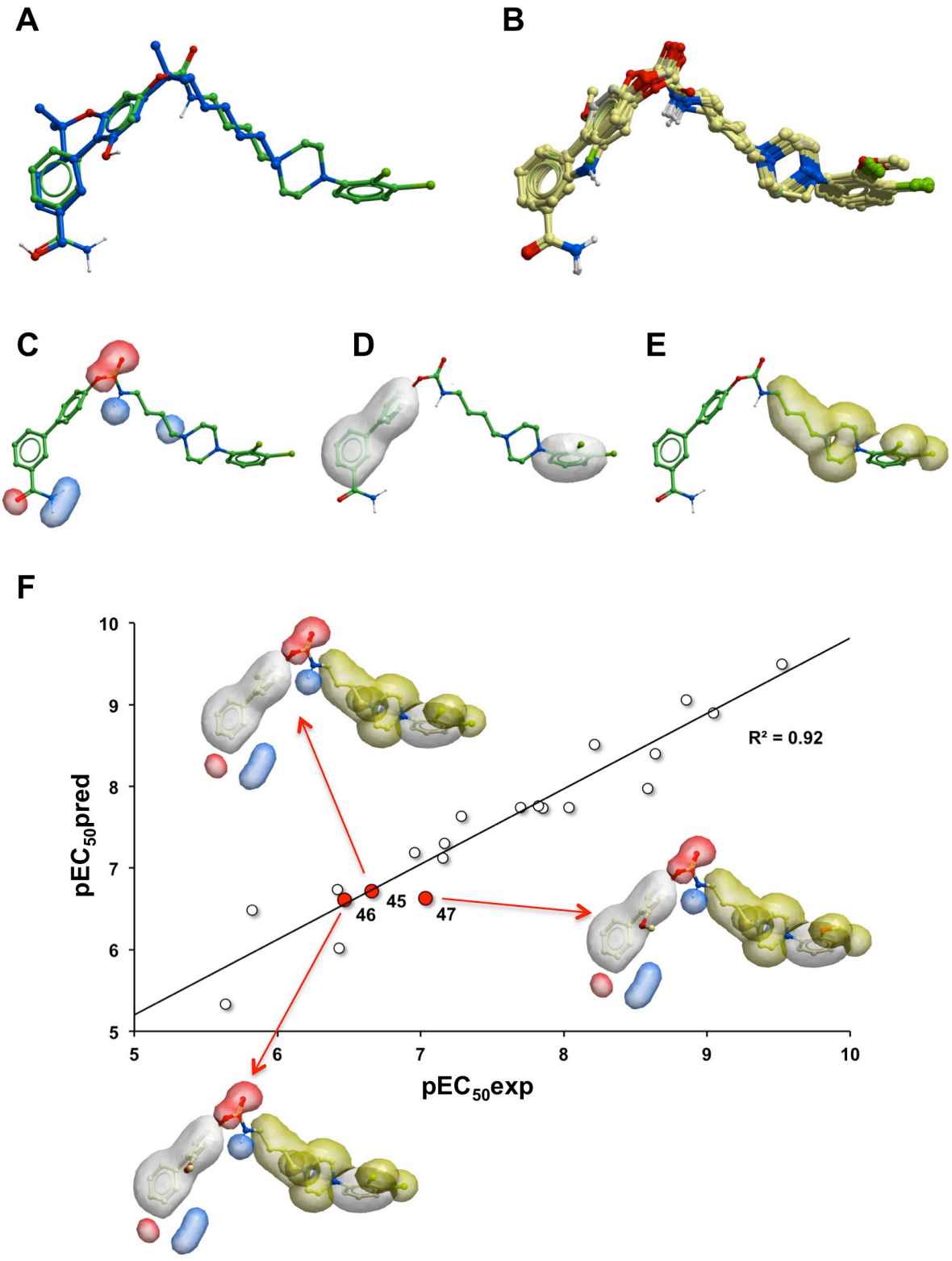
A
B
C
D
E
F
10
9
8
7
6
5
5
6
7
8
9
10
pEC50pred
pEC50exp
R² = 0.92
45
46
47

Figure 5. Computational studies to rationalize activity at CB_1R. A) APF-based superimposition of **4** and **39**, using the putative receptor-bound conformation of the latter as a rigid template; B) 3D alignment of the 18 molecules included in the training set; C) Equipotential contours of the H-bond acceptor (red) and H-bond donor (blue) APF components; D) Equipotential contours of the sp2 carbon atom hybridization APF component (white); E) Equipotential contours of the lipophilicity APF component (green); F) Correlation plot between pIC50exp and pIC50pred. The structures of the predicted compounds (red dots) are reported explicitly.

3D-QSAR Studies. At this point, we attempted a 3D-QSAR analysis to systematically describe, at the structural level, the CB_1 R activity in our series and to prospectively test our hypothesis. This 3D-QSAR analysis was carried out by means of the Atom Property Fields (APF) methods originally developed by Totrov (see Experimental Section for details).[46] A set of 18 molecules, encompassing **2**-**4, 16**-**17**, **21-24**, **27**, **29**-**33**, and **42**-**44**, namely all molecules which had been tested for CB_1R activity, were automatically aligned to the previously generated conformation of **4** (Figure 5B). For each molecule, we generated a set of seven three-dimensional continuous potentials, representative of seven molecular properties (namely, presence of a hydrogen bond donor, presence of a hydrogen bond acceptor, sp^2 carbon atom hybridization, charge, lipophilicity, size and electropositivity/negativity), approximated on a set of regularly spaced grids. Each molecule could thus be expressed by 126 descriptors: the pseudo-energy values generated by the molecule's fit in each of the 7 property fields of the 18 compounds in the training set. Each descriptor was assigned a weight by means of a partial least square (PLS) fitting procedure in order to reproduce experimental activity data. Eventually, we selected 4 latent vectors (see Table 3).

Table 3. Squared correlation coefficients (R^2) and leave-one-out squared correlation coefficients (Q^2) according to the number of latent vectors.

No. of latent vectors	R^2	RMSE[a]	Q^2_{LOO}[b]	$RMSE_{LOO}$[b]
1	0.10	1.04	0.05	1.1
2	0.82	0.46	0.74	0.54
3	0.87	0.39	0.74	0.57
4	0.92	0.30	0.79	0.51
5	0.94	0.26	0.82	0.46
6	0.95	0.24	0.82	0.46
7	0.97	0.19	0.82	0.47
8	0.98	0.15	0.83	0.46
9	0.99	0.10	0.81	0.48
10	0.99	0.09	0.81	0.48\

[a] Root Mean Squared Error; [b] Leave-one-out;

According to best practice, selecting roughly one latent vector for every 5 compounds in the training set is a good heuristic ratio for building the model in order to avoid overfitting and to achieve external validity.[48] Furthermore, in this specific case, including more latent vectors would not have substantially increased our model's predictive power within the set (Table 3). By

combining the activity-weighted maps from individual compounds, we can identify two key features conducive to CB_1R activity: i) the presence of a hydrogen bond donor/acceptor in the distal phenyl ring of the biphenyl group (Figure 5C) and ii) an extended and not completely flat ring system (Figure 5D). This is consistent with our previously reported findings that compounds bearing a naphthyl group at the *O*-side of the carbamate display much lower CB_1R activities. Given the structural homogeneity of the training set, other features (such as the hydrogen bond donor/acceptor signal in carbamate region or the strong lipophilic signal generated by the aryl-piperazine tail (Figure 5E)) are consistent with the data but not very informative. Table 4 reports the experimental (pEC_{50ex}), predicted (pEC_{50pred}), and leave-one-out cross-validated ($pEC_{50l.o.o.}$) pEC_{50} values for the training set.

Table 4. Experimental, Predicted, and Leave-One-Out Cross-Validated pEC_{50} Values for the Training Set Compounds

Compound	pEC_{50exp}	pEC_{50pred}	pEC_{50LOO}
2	9.04	8.90	8.72
3	9.52	9.50	9.36
4	7.85	7.73	7.71
16	8.85	9.06	9.18
17	8.64	8.40	8.23
21	8.21	8.51	8.68

22	8.58	7.98	7.50
23	7.17	7.30	7.35
24	7.28	7.63	7.72
27	7.82	7.76	7.76
29	6.96	7.19	7.36
30	7.70	7.74	7.67
31	8.04	7.74	7.32
32	7.15	7.12	6.91
33	5.82	6.48	6.70
42	6.42	6.73	7.01
43	6.43	6.02	5.75
44	5.63	5.33	5.10

The model was internally very consistent with a R^2 equal to 0.92 (Figure 5F) and a root mean squared error (RMSE) of 0.30. No compound emerged as a clear outlier. The leave-one-out (LOO) procedure for cross-validation returned a still predictive Q^2 of 0.79 (RMSE 0.51, Table 3).

Again, no predicted activity departed by more than one order of magnitude from the experimental value.

Prospective validation of the 3D-QSAR model. Finally, in order to prospectively challenge our hypothesis and confirm that the SAR for classic CB_1R agonists applies to our molecules, we designed three novel compounds and used the APF–based 3D-QSAR model to predict their activities at the CB_1R receptor. This is particularly relevant because our model was generated from a limited number of molecules. Our design concept for compounds **45**-**47** was to introduce small structural variations of **33** in order to retain its selectivity against CB_1R, avoiding hydrogen bond donor/acceptor groups in the distal biphenyl ring while introducing substitutions in the proximal one (see Table 5).

Table 5. Biological data of 3D-QSAR predicted and synthesized molecules

Structure											
						Predicted CB_1	Experimental CB_1	Experimental CB_1	Human FAAH	D3R	D3R %
Compound	R_1	R_2	X	R_3	R_4	pEC_{50}	EC_{50} (nM)	pEC_{50}	IC_{50} (nM)[a]	EC_{50} (nM)	efficacy[b]
45 (19679)	Cl	Cl	CH_2CH_2	OMe	H	6.64	220	6.66	4.3±1.3	1.66	32
46 (19659)	Cl	Cl	CH_2CH_2	F	H	6.55	340	6.47	6.0±0.8	3.7	40
47 (16050)	H	OMe	CH_2CH_2	OMe	H	6.50	93	7.03	43.0±12.0	37	80

[a] n=3; [b] as of 300 nM of dopamine;

Substitutions in the proximal ring: i) are generally well-tolerated in FAAH and help improve the solubility profile[34] and ii) are detrimental for CB_1R activity when coupled with a lack of hydrogen bond donor/acceptor groups (Table 1). Figure 5F reports the fitting of **45**-**47** in the global APF maps generated by the molecules of the training set. We then synthesized and tested these compounds. Predictions were generally in good agreement with the experimental data (red circles in Figure 5F). For **45** and **46**, the experimental activities matched the predictions remarkably well. Furthermore, these two molecules were endowed with potent and balanced activities at the main targets with a clear partial agonist profile at D3R. Although their affinity for CB_1R increased with respect to **33**, the selectivity profile remained acceptable thanks to these potency values, and actually improved in **46**. In **47**, while still rather accurate, the model suggested a slightly less potent molecule (pEC_{50pred} equal 6.50) than the experimental result (pEC_{50pred} equal 7.03, Table 5). Here, the selectivity with respect to CB_1R was also compromised by decreased potency at the main targets.

Preliminary pharmacokinetics characterization and selectivity profiling of 33. Given its promising activity at the main targets, its physico-chemical profile (molecular weight: 498; polar surface area: 46.1; calculated logP: 5.48), and its selectivity profile at off targets known from previous studies, we selected **33** as the new lead compound for further pharmacokinetics (PK) studies and selectivity profile characterization. First, we assessed how **33** remained stable in rat plasma for over an hour with an average $t_{½}$ of 97±13 min (n=3). The compound was also stable in rat liver microsomes ($t_{½}$ > 60 min, n=3). PK analyses in rats showed that **33** possessed good oral bioavailability and blood-brain barrier (BBB) penetration. After dosing **33** intravenously and orally, we monitored plasma concentrations for 8 hours. After intravenous dosing (3 mg kg^{-1}), we measured a maximal plasma concentration of 500 ng ml^{-1} (5 minutes time point). The half-life of

33 for the elimination phase was 145 minutes. Compound **33** showed a volume of distribution of 23.7 l kg^{-1} and disappeared from the systemic circulation with a clearance of 0.11 l min^{-1} kg^{-1}. After oral administration (10 mg kg^{-1}), the maximal plasma concentration of **33** (54 ng ml^{-1}) was observed 120 minutes after dosing. The oral bioavailability of **33** was 21%. BBB penetration of this compound was also measured for the *per os* arm of the study (10 mg ml^{-1}): **33** reached a maximum concentration of 37 ng ml^{-1} of brain homogenate, 4 hours after oral administration; the total brain exposure (AUC) was quantified in 84.5 $ng_{*}min$ ml^{-1} (see also Figure S1 in the Supporting Information). It can be calculated that **33** reaches a total brain concentration of approximately 391 nM, more than adequate to effectively engage the target (see SI for details).

In terms of selectivity, we reasoned that CB_1R and D2R were off targets selected based on the compound's alleged mechanism of action. Next, we decided to begin expanding the polypharmacological profile of **33** investigating its activity at off targets selected based on the compound structure. Displaying an aryl-piperazine, which is a privileged moiety for interacting with aminergic receptors,[49] we tested the activity of **33** at this class of GPCRs starting from beta adrenergic receptors subtype β_1 and β_2 and serotonergic receptor subtypes 5-HT_{1A} and 5-HT_{1b}. In binding experiments, **33** turned out to be selective with respect to both beta adrenergic receptor subtypes and 5-HT_{1b}. Interestingly a moderate affinity for 5-HT_{1A} could be detected (60.4% inhibition of the binding of a labelled radioligand at 100 nM, see Supporting Information for details). On the same line, as **33** bears an aryl carbamate, which is a warhead exploited by several compounds to interact with hydrolases, we tested **33** for activity at monoacylglycerol lipase (MAGL). We selected this classic serine hydrolase since it is responsible for over 80% of the degradation of 2-arachidonoylglycerol (2-AG), another key mediator together with AEA in the cannabinoid transmission.[50] Based on high-resolution mass spectrometry data, we were able

to conclude that **33** exert irreversible covalent inhibition at FAAH but not at MAGL. Experimental details are reported in the Supporting Information. While further studies will be necessary to describe the complete pharmacological fingerprint of **33**, and possibly other members of this series, it is tempting to speculate that this class of compounds could share some common features with the structurally related antipsychotic drug aripiprazole, which has been recently investigated for the treatment of addiction.[51]

CONCLUSIONS

In this study, we conducted the first exploration of the SAR of a series of biphenyl-N-[4-[4-(2,3-substituted-phenyl)piperazine-1-yl]alkyl]carbamates. Within the MTDL framework, these molecules were purposely designed to exert a combined activity at the FAAH enzyme and the D3 receptor. Ideally, the concurrent modulation of these two targets should produce an enhanced therapeutic profile for treating addiction (in particular, nicotine addiction) and compulsive behaviors in general. We have rationalized the structural features conducive to activities at the main targets and we have investigated activities at two off-targets, D2R and CB_1R. In light of structural insights previously reported by other authors, it was quite straightforward to explain activity at (and selectivity over) D2R. In contrast, concerted modeling and synthetic efforts were required to understand the remarkable affinity for CB_1R displayed by our first set of biphenyl derivatives. Using a prospectively validated 3D-QSAR model, we proposed that our molecules behave like classic THC-based CB_1R agonists. This knowledge could be used to design out unwanted affinity at CB_1R. One derivative, **33**, was endowed with quite balanced affinities for the two targets and was fairly selective over the two off-targets. This molecule was stable in plasma and in the presence of rat liver microsomes. Upon oral administration, **33** showed moderate oral bioavailability and crossed the blood-brain barrier. In light of these results, we

conclude that this class of compounds has potential for further development. Future efforts will be devoted to: i) assessing the effects of more radical structural variations on the original scaffold, ii) carrying out a much broader characterization of off-target activities,[52] including other dopamine receptor subtypes, monoamine receptors and transporters, and hERG, and iii) testing the efficacy of these compounds in in vivo models of nicotine addiction and other compulsive behaviors.

EXPERIMENTAL SECTION

a. Chemistry

Chemicals, materials, and methods. Abbreviations used in the description of the examples that follow are: Acetonitrile (MeCN); ammonium chloride (NH_4Cl); BnBr (benzyl bromide); carbonyldiimidazole (CDI); cesium carbonate (Cs_2CO_3); cyclohexane (Cy); chloroform ($CHCl_3$); deuterated chloroform ($CDCl_3$ or Chloroform-*d*); deuterated dimethylsulfoxyde (DMSO-*d6*); dichloromethane (DCM); dimethylsulfoxyde (DMSO); N,N-diisopropylethylamine (DIPEA); dimethylacetamide (DMA); di-tert-butyldicarbonate (Boc_2O); 4-(dimethylamino)-pyridine (DMAP); ethylene glycol monomethyl ether (EGME); ethanol (EtOH); electrospray (ES); ethyl acetate (EtOAc); hydrochloric acid (HCl); mass spectrometry (MS); microwave (MW); sulfuric acid (H_2SO_4); iodomethane (MeI); N,N-dimethylformamide (DMF); lithium hydroxide (LiOH); magnesium sulphate (MgSO4); methanol (MeOH); nuclear magnetic resonance (NMR); room temperature (RT); palladium acetae ($Pd(OAc)_2$); potassium carbonate (K_2CO_3); sodium bicarbonate ($NaHCO_3$); tetrabutylammonium iodide (TBAI); triethylsilane (TES); tetrahydrofurane (THF); thin layer chromatography (TLC); and triethylamine (Et_3N); trifluoroacetic acid (TFA).

Automated column chromatography purifications were conducted using a Teledyne ISCO apparatus (CombiFlashTM Rf) with prepacked silica gel columns of different sizes (from 4 g until 120 g). Mixtures of increasing polarity of cyclohexane and ethyl acetate or dichloromethane and methanol were used as eluents. Preparative TLCs were performed using Macherey-Nagel pre-coated 0.05 mm TLC plates (SIL G-50 UV254). Hydrogenation reactions were performed using H-Cube^{TM} continuous hydrogenation equipment (SS-reaction line version), using disposable catalyst cartridges (CatCartTM) preloaded with the required heterogeneous catalyst. Microwave heating was performed using ExplorerTM-48 positions instrument (CEM). NMR experiments were run on a Bruker Avance III 400 system (400.13 MHz for ^{1}H, and 100.62 MHz for ^{13}C), equipped with a BBI probe and Z-gradients. Spectra were acquired at 300 K, using deuterated dimethylsulfoxyde (DMSO-*d6*) or deuterated chloroform (CDCl3) as solvents. Chemical shifts for ^{1}H and ^{13}C spectra were recorded in parts per million using the residual non-deuterated solvent as the internal standard (for CDCl3: 7.26 ppm, ^{1}H and 77.16 ppm, ^{13}C; for DMSO-*d6*: 2.50 ppm, ^{1}H; 39.52 ppm, ^{13}C).

UPLC/MS analyses were run on a Waters ACQUITY UPLC/MS system consisting of a SQD (Single Quadrupole Detector) Mass Spectrometer equipped with an Electrospray Ionization interface and a Photodiode Array Detector. PDA range was 210-400 nm. Electrospray ionization was applied in positive and negative mode. UPLC mobile phases were: (A) 10mM NH_4OAc in H_2O, pH 5; (B) 10mM NH_4OAc in MeCN/H_2O (95:5), pH 5. Analyses were performed with either method A, B, or C as reported below.

Method A (generic):

Gradient: 5 to 95% B over 3 min. Flow rate 0.5 mL/min. Temp. 40 °C

Pre column: Vanguard BEH C18 (1.7µm 2.1x5mm). Column: BEH C18 (1.7µm 2.1x50mm)

Method B (polar):

Gradient: 0 to 50% B over 3 min. Flow rate 0.5 mL/min. Temp. 40 °C

Pre column: VanGuard HSS T3 C18 (1.7µm 2.1x5 mm). Column HSS T3 (1.8µm 2.1x50mm)

Method C (apolar):

Gradient: 50 to 100% B over 3 min. Flow rate 0.5 mL/min. Temp. 40 °C

Pre column: Vanguard BEH C18 (1.7µm 2.1x5mm). Column: BEH C18 (1.7µm 2.1x50mm)

Purifications by preparative HPLC/MS were run on a Waters Autopurification system consisting of a 3100 Single Quadrupole Mass Spectrometer equipped with an Electrospray Ionization interface and a 2998 Photodiode Array Detector. The HPLC system included a 2747 Sample Manager, 2545 Binary Gradient Module, System Fluidic Organizer and 515 HPLC Pump. PDA range was 210-400 nm. Purifications were performed on an XBridgeTM Prep C18 OBD column (100x19mmID, particle size 5µm) with an XBridgeTM Prep C18 (10x19mmID, particle size 5µm) Guard Cartridge. Mobile phases were 10mM NH_4OAc in H_2O at pH 5 adjusted with AcOH (A) and 10mM NH_4OAc in MeCN-H_2O (95:5) at pH 5 (B). Electrospray ionization was used in positive and negative mode. Analyses by chiral HPLC were run on a Waters Alliance HPLC instrument consisting of an e2695 Separation Module and a 2998 Photodiode Array Detector. PDA range was 210-400 nm. Analyses were performed isocratically on a Daicel ChiralPak AD column (250x4.6mmID, particle size 10µm). Mobile phase was 0.1% TFA Heptane-2-Propanol (75:25). Separations by preparative chiral HPLC were run on a Waters Alliance HPLC instrument consisting of a 1525 Binary HPLC Pump, Waters Fraction Collector III, and a 2998 Photodiode Array Detector. UV detection was at 240 nm. Purifications were

performed isocratically on a Daicel ChiralPak AD column (250x10mmID, particle size 10µm). Mobile phase was 0.1% TFA Heptane-2-Propanol (75:25).

General Procedure 1 for the synthesis of the arylpiperazine amine derivatives 7a-j (Scheme 1)

Step A.

A mixture of aryl piperazine.HCl (1 eq.), N-(bromoalkyl)phthalimide (1.1 eq.), and base (K_2CO_3 or triethylamine, 3 eq.) in acetonitrile was heated to reflux for 6 hours. The hot suspension was filtered and the residue washed with acetone several times. The filtrates were concentrated under reduced pressure to give the phthalimide intermediates.

Step B.

The phthalimide derivative (1 eq.) and hydrazine hydrate (1.2 eq.) in methanol were heated to reflux for 2 hours. To the hot solution was added 2N HCl, and reflux was continued for one more hour. After cooling to ambient temperature, the mixture was filtrated, the residue washed with methanol, and the filtrate evaporated to dryness. This residue was suspended in water and neutralized with 2N NaOH. Extraction with EtOAc afforded an oily product, which was pure enough for the next step.

General Procedure 2 for the synthesis of phenolic derivatives 9a-h (Scheme 2)

Commercially available aryl boronic acid derivative (1.2 eq.) was added to a solution of the appropriate aryl halide (1 eq.) in EGME/water 3:1, followed by the addition of $Pd(OAc)_2$ (0.01 eq.) and K_2CO_3 (2.5 eq.). After a few minutes, the yellowish suspension turned dark-black and the reaction reached full conversion. The mixture was stirred for a further 5 min., then diluted with water, acidified with 2N HCl, and extracted with DCM. The organic phase was dried over

Na_2SO_4 and concentrated to dryness. The crude residue was adsorbed on silica and purified by flash chromatography (Eluent: 5% MeOH in DCM).

General Procedure 3 for the synthesis of the final carbamate derivatives (Scheme 1)

Method A.

To a solution of di-*tert*-butyldicarbonate (1.4 eq.) in acetonitrile were added in sequence: a solution of DMAP (1 eq.) in acetonitrile and a solution of the appropriate amine (1 eq.) in acetonitrile. After stirring for 10 minutes at room temperature, the alcohol derivative (1.2-1.4 eq.) was added. The reaction mixture was stirred for 23 hours at room temperature, after which the solvent was evaporated under reduced pressure. The crude residue was solubilized in ethyl acetate and washed with a saturated solution of $NaHCO_3$. The organic layer was dried (Na_2SO_4), concentrated and purified by flash chromatography (Eluent: 5% MeOH in DCM).

Method B.

The amine derivative (1.0 eq.) was treated with *p*-nitrophenylchloroformate (1.1 eq.) and DIPEA (1.1 eq.) in a 1:1 mixture of DMA:DCM. The reaction mixture was stirred at ambient temperature for 30 minutes. To the resulting *p*-nitrophenyl carbamate solution were added the alcohol derivative (1.25 eq.) and DIPEA (1.1 eq., 2.2 total) and the resultant mixture was stirred at room temperature overnight. The desired carbamate was isolated by removal of the undesired *p*-nitrophenol byproduct and DMA by washing several times with brine and water, collection and concentration of the organic phase and purification by flash chromatography (Eluent: 5% MeOH in DCM).

[3-(3-carbamoylphenyl)phenyl] N-[3-[4-(2-methoxyphenyl)piperazin-1-yl]propyl] carbamate (16)

The title compound was synthesized according to the general procedure 3 Method A, starting from di-*tert*-butyldicarbonate (115 mg, 0.53 mmol), 4-dimethylaminopyridine (64 mg, 0.53 mmol) 3-[4-(2-methoxyphenyl)piperazin-1-yl]propan-1-amine (120 mg, 0.48 mmol), and 3-(3-hydroxyphenyl)benzamide (112 mg, 0.53 mmol) in acetonitrile (4 mL). White solid 70 mg (30%). mp: 91-95 °C. UPLC-MS (method A): Rt 1.88 min, m/z 489 $[M+H]^+$. ^{1}H NMR (400 MHz, DMSO-d_6) δ 8.18 – 8.14 (m, 1H), 8.14 – 8.07 (m, 1H), 7.90 – 7.85 (m, 1H), 7.85 – 7.79 (m, 2H), 7.61 – 7.46 (m, 4H), 7.45 – 7.38 (m, 1H), 7.17 – 7.11 (m, 1H), 6.96 – 6.83 (m, 4H), 3.76 (s, 3H), 3.14 (q, J = 6.8 Hz, 2H), 2.96 (s, 4H), 2.55 – 2.46 (m, 4H), 2.39 (t, J = 7.0 Hz, 2H), 1.68 (p, J = 7.1 Hz, 2H). ^{13}C NMR (101 MHz, DMSO) δ 167.79, 157.87, 154.31, 151.96, 141.27, 140.26, 139.20, 134.97, 129.26, 128.83, 126.96, 126.52, 125.60, 123.35, 122.30, 121.16, 120.83, 120.16, 117.87, 111.91, 55.62, 55.30, 53.03 (2C), 50.05 (2C), 39.01, 26.47. ESI+ (m/z): $[M+H]^+$ calculated for C_{28} H_{32} N_4 O_4 489,2475; found: 489,2494 $[M+H]^+$. UPLC-MS Purity (UV @ 215 nm): 99%.

[3-(3-carbamoylphenyl)phenyl] N-[4-[4-(2-methoxyphenyl)piperazin-1-yl]butyl] carbamate (17)

The title compound was synthesized according to the general procedure 3 Method A, starting from di-*tert*-butyldicarbonate (153 mg, 0.70 mmol), 4-dimethylaminopyridine (61 mg, 0.50 mmol) 4-[4-(2-methoxyphenyl)piperazin-1-yl]butan-1-amine (132 mg, 0.50 mmol), and 3-(3-hydroxyphenyl)benzamide (150 mg, 0.70 mmol) in acetonitrile (4 mL). White solid 51 mg (20%). mp: 90-94 °C. UPLC-MS (method A): Rt 1.90 min; m/z 503 [M+H]+. ^{1}H NMR (400 MHz, DMSO-d_6) δ 8.19 – 8.14 (m, 1H), 8.12 (br. s, 1H), 7.90 – 7.79 (m, 3H), 7.60 – 7.46 (m, 4H), 7.42 (br. s, 1H), 7.16 – 7.10 (m, 1H), 6.96 – 6.83 (m, 4H), 3.76 (s, 3H), 3.18 – 3.06 (m, 2H), 3.04 – 2.88 (m, 4H), 2.57 – 2.44 (m, 4H), 2.39 – 2.26 (m, 2H), 1.62 – 1.42 (m, 4H). ^{13}C NMR

(101 MHz, DMSO-d_6) δ 168.96, 157.54, 152.44, 150.49, 140.92, 140.68, 140.07, 132.79, 129.74, 128.83, 128.75, 126.62, 126.12, 122.44, 122.36, 119.69, 118.35, 117.71, 114.35, 56.72, 56.42, 52.27, 49.82, 40.36, 27.50, 25.56. ESI+ (m/z): $[M+H]^+$ calculated for C_{29} H_{34} N_4 O_4 503,2658; found 503,2667 $[M+H]^+$. UPLC-MS Purity (UV @ 215 nm): 99%.

[3-(3-carbamoylphenyl)phenyl] N-[3-(4-phenylpiperazin-1-yl)propyl]carbamate (18)

The title compound was synthesized according to the general procedure 3 Method A, starting from di-*tert*-butyldicarbonate (167 mg, 0.77 mmol), 4-dimethylaminopyridine (67 mg, 0.55 mmol), 3-(4-phenylpiperazin-1-yl)propan-1-amine (120 mg, 0.55 mmol), and 3-(3-hydroxyphenyl)benzamide (140 mg, 0.66 mmol) in acetonitrile (4 mL). White solid 40 mg (16%). mp: 176-178 °C. UPLC-MS (method A): Rt 1.94 min; m/z 459 $[M-H]^+$. ^{1}H NMR (400 MHz, DMSO-d_6) δ 8.19 – 8.14 (m, 1H), 8.12 (br. s, 1H), 7.91 – 7.85 (m, 1H), 7.85 – 7.78 (m, 2H), 7.61 – 7.46 (m, 4H), 7.42 (br. s, 1H), 7.23 – 7.16 (m, 2H), 7.16 – 7.10 (m, 1H), 6.95 – 6.88 (m, 2H), 6.80 – 6.73 (m, 1H), 3.19 – 3.09 (m, 6H), 2.54 – 2.51 (m, 4H), 2.39 (t, J = 7.1 Hz, 2H), 1.69 (p, J = 7.1 Hz, 2H). ^{13}C NMR (101 MHz, DMSO) δ 167.67, 154.28, 151.68, 151.01, 140.77, 139.18, 134.96, 129.78, 129.40, 128.97, 128.85 (2C), 126.94, 125.59, 123.33, 121.13, 120.14, 118.68, 115.26 (2C), 55.25, 52.73 (2C), 48.20 (2C), 39.32, 26.46. ESI+ (m/z): $[M+H]^+$ calculated for C_{27} H_{30} N_4 O_3 459,2396; found 459,2409 $[M+H]^+$. UPLC-MS Purity (UV @ 215 nm): 98%.

[3-(3-carbamoylphenyl)phenyl] *N*-[4-(4-phenylpiperazin-1-yl)butyl]carbamate (19)

The title compound was synthesized according to the general procedure 3 Method A, starting from di-*tert*-butyl dicarbonate (550 mg, 2.52 mmol), DMAP (264 mg, 2.16 mmol), 4-(4-phenylpiperazin-1-yl)butan-1-amine (420 mg, 1.8 mmol), and 3-(3-hydroxyphenyl)benzamide (460 mg, 2.16 mmol) in CH_3CN (4 mL). White solid 504 mg (59%). mp: 176-178 °C. UPLC-MS

(method A): Rt 1.77 min; m/z 473 $[M+H]^+$. ^{1}H NMR (600 MHz, DMSO-d_6) δ 8.16 (t, J = 1.8 Hz, 1H), 8.13 (br. s, 1H), 7.90 – 7.84 (m, 2H), 7.82 (dt, J = 7.8, 1.4 Hz, 1H), 7.60 – 7.52 (m, 2H), 7.51 – 7.46 (m, 2H), 7.44 (br. s, 1H), 7.22 – 7.17 (m, 2H), 7.12 (dd, J = 8.0, 2.4 Hz, 1H), 6.91 (d, J = 8.2 Hz, 2H), 6.76 (t, J = 7.2 Hz, 1H), 3.16 – 3.08 (m, 6H), 2.56 – 2.49 (m, 4H), 2.37 – 2.30 (m, 2H), 1.56 – 1.48 (m, 4H). ^{13}C NMR (151 MHz, DMSO) δ 167.68, 154.34, 151.72, 151.06, 140.80, 139.21, 134.98, 129.84, 129.46, 129.03, 128.90 (2C), 126.99, 125.62, 123.38, 121.21, 120.20, 118.73, 115.30 (2C), 57.50, 52.77 (2C), 48.19 (2C), 40.18, 27.25, 23.62. ESI+ (m/z): $[M+H]^+$ calculated for C_{27} H_{30} N_4 O_3 459,2396; found 459,2409 $[M+H]^+$. UPLC-MS Purity (UV @ 215 nm): 98%.

(3-phenylphenyl) N-[4-[4-(2,3-dichlorophenyl)piperazin-1-yl]butyl]carbamate hydrochloride (20)

The title compound was synthesized according to the general procedure 3 Method A, starting from di-*tert*-butyldicarbonate (111 mg, 0.51 mmol), 4-dimethylaminopyridine (53 mg, 0.44 mmol) 4-[4-(2,3-dichlorophenyl)piperazin-1-yl]butan-1-amine (110 mg, 0.36 mmol), and 3-phenylphenol (68 mg, 0.40 mmol) in acetonitrile (4 mL). The compound was isolated as hydrochloride salt. White solid 52 mg (27%). mp: 91-95 °C. UPLC-MS (method A): Rt 3.12 min, m/z 498 $[M+H]^+$. ^{1}H NMR (400 MHz, DMSO-d_6) δ 11.15 (br. s, 1H), 7.89 (t, J = 5.7 Hz, 1H), 7.70 – 7.63 (m, 2H), 7.53 – 7.43 (m, 4H), 7.41 – 7.32 (m, 4H), 7.19 (dd, J = 7.0, 2.6 Hz, 1H), 7.14 – 7.10 (m, 1H), 3.62 – 3.55 (m, 2H), 3.47 – 3.40 (m, 2H), 3.30 – 3.08 (m, 8H), 1.89 – 1.73 (m, 2H), 1.55 (p, J = 7.5 Hz, 2H). ^{13}C NMR (101 MHz, DMSO) δ 154.43, 151.63, 149.56, 141.46, 139.28, 138.98, 132.76, 129.80, 129.00, 128.67, 127.78, 126.74, 126.08, 125.31, 123.27, 120.82, 119.96, 119.81, 106.96, 55.09, 51.05 (2C), 47.67 (2C), 39.40, 26.44, 20.48 ESI+ (m/z):

$[M+H]^+$ calculated for C_{27} H_{29} Cl_2 N_3 O_2 · Cl H 498,1722; found 498,1721 $[M+H]^+$. UPLC-MS Purity (UV @ 215 nm): 96%.

[4-(3-carbamoylphenyl)phenyl] N-[3-[4-(2,3-dichlorophenyl)piperazin-1-yl] propyl]carbamate (21)

The title compound was synthesized according to the general procedure 3 Method A, starting from di-*tert*-butyldicarbonate (85 mg, 0.39 mmol), 4-dimethylaminopyridine (34 mg, 0.28 mmol), 3-[4-(2,3-dichlorophenyl)piperazin-1-yl]propan-1-amine (80 mg, 0.28 mmol), and 3-(4-hydroxyphenyl)benzamide (83 mg, 0.39 mmol) in acetonitrile (4 mL). White solid 34 mg (23%). mp: 176-178 °C. UPLC-MS (method A): Rt 2.34 min; m/z 527 $[M-H]^+$. ^{1}H NMR (400 MHz, DMSO-d_6) δ . 8.14 (t, J = 1.8 Hz, 1H), 8.08 (br. s, 1H), 7.87 – 7.83 (m, 1H), 7.82 – 7.77 (m, 2H), 7.76 – 7.70 (m, 2H), 7.54 (t, J = 7.7 Hz, 1H), 7.40 (br. s, 1H), 7.34 – 7.27 (m, 2H), 7.25 – 7.19 (m, 2H), 7.15 (dd, J = 6.6, 3.0 Hz, 1H), 3.14 (q, J = 6.6 Hz, 2H), 3.05 – 2.95 (m, 4H), 2.62 – 2.52 (m, 4H), 2.42 (t, J = 7.1 Hz, 2H), 1.69 (p, J = 7.0 Hz, 2H). ^{13}C NMR (101 MHz, DMSO) δ 167.90, 157.35, 151.18, 134.79, 132.58, 130.25, 129.24, 128.71, 128.58, 128.39, 127.87 (2C), 127.67, 125.49, 124.88, 124.27, 122.20 (2C), 119.49, 115.73, 55.44, 52.83 (2C), 50.91 (2C), 39.07, 27.21. ESI+ (m/z): $[M+H]^+$ calculated for C_{27} H_{28} Cl_2 N_4 O_3 527,1617; found 527,1612 $[M+H]^+$. UPLC-MS Purity (UV @ 215 nm): 98%.

[4-(3-carbamoylphenyl)phenyl] N-[3-[4-(2-methoxyphenyl)piperazin-1-yl] propyl]carbamate (22)

The title compound was synthesized according to the general procedure 3 Method B, starting from *p*-nitrophenylchloroformate (104 mg, 0.52 mmol), DIPEA (0.15 mL, 0.84 mmol), 3-[4-(2-methoxyphenyl)piperazin-1-yl]propan-1-amine (70 mg, 0.47 mmol), and 3-(4-hydroxyphenyl)benzamide (100 mg, 0.47 mmol) in a 1:1 mixture of DMA:DCM (4 mL). White

solid 22 mg (10%). mp: 91-95 °C. UPLC-MS (method A): Rt 1.83 min; m/z 489 $[M-H]^+$. ^1H NMR (400 MHz, DMSO-d_6) δ 8.14 (t, 1H), 8.09 (br. s, 1H), 7.88 – 7.84 (m, 1H), 7.83 – 7.78 (m, 2H), 7.76 – 7.70 (m, 2H), 7.54 (t, J = 7.7 Hz, 1H), 7.41 (br. s, 1H), 7.26 – 7.20 (m, 2H), 6.97 – 6.82 (m, 4H), 3.77 (s, 3H), 3.14 (q, J = 6.7 Hz, 2H), 3.04 – 2.90 (m, 4H), 2.60 – 2.51 (m, 4H), 2.39 (t, J = 7.1 Hz, 2H), 1.68 (p, J = 7.0 Hz, 2H). ^{13}C NMR (101 MHz, DMSO-d_6) δ 168.96, 157.54, 154.16, 150.49, 140.92, 140.89, 134.01, 133.02, 129.15, 128.85, 128.82, 126.42, 125.87, 122.36, 120.04, 119.69, 117.71, 114.35, 56.42, 54.54, 52.27, 49.82, 37.82, 24.56. ESI+ (m/z): $[M+H]^+$ calculated for $C_{28}H_{32}N_4O_4$ 489,2502; found 489,2507 $[M+H]^+$. UPLC-MS Purity (UV @ 215 nm): 98%.

[4-(3-carbamoylphenyl)phenyl] N-[4-[4-(2-methoxyphenyl)piperazin-1-yl]butyl] carbamate (23)

The title compound was synthesized according to the general procedure 3 Method B, starting from *p*-nitrophenylchloroformate (84 mg, 0.42 mmol), DIPEA (0.15 mL, 0.84 mmol), 4-[4-(2-methoxyphenyl)piperazin-1-yl]butan-1-amine (100 mg, 0.38 mmol), and 3-(4-hydroxyphenyl)benzamide (101 mg, 0.47 mmol) in a 1:1 mixture of DMA:DCM (4 mL). White solid 50 mg (26%). mp: 91-95 °C. UPLC-MS (method A): Rt 1.86 min; m/z 503 $[M-H]^+$. ^1H NMR (400 MHz, DMSO-d_6) δ 10.95 (br. s, 1H), 8.29 – 7.99 (m, 2H), 7.95 – 7.77 (m, 3H), 7.77 – 7.69 (m, 2H), 7.54 (t, J = 7.7 Hz, 1H), 7.41 (br. s, 1H), 7.29 – 7.19 (m, 2H), 7.08 – 6.87 (m, 4H), 3.79 (s, 3H), 3.51 (dd, J = 18.6, 10.4 Hz, 4H), 3.22 – 3.04 (m, 8H), 1.89 – 1.74 (m, 2H), 1.54 (p, J = 7.2 Hz, 2H). ^{13}C NMR (101 MHz, DMSO) δ 167.74, 154.31, 151.82, 150.86, 139.42, 139.29, 136.30, 134.94, 129.27, 128.93, 127.70 (2C), 126.49, 125.57, 123.54, 122.23 (2C), 120.85, 118.28, 111.97, 55.39, 55.08, 51.03 (2C), 46.85 (2C), 39.71, 26.43, 20.48. ESI+ (m/z): $[M+H]^+$

calculated for $C_{29}H_{34}N_4O_4$ 503,2658; found 503,2665 $[M+H]^+$. UPLC-MS Purity (UV @ 215 nm): 98%.

[4-(3-carbamoylphenyl)phenyl] N-[4-[4-(o-tolyl)piperazin-1-yl]butyl]carbamate (24)

The title compound was synthesized according to the general procedure 3 Method A, starting from di-*tert*-butyldicarbonate (136 mg, 0.62 mmol), 4-dimethylaminopyridine (65 mg, 0.53 mmol) 4-[4-(o-tolyl)piperazin-1-yl]butan-1-amine (110 mg, 0.44 mmol), and 3-(4-hydroxyphenyl)benzamide (83 mg, 0.38 mmol) in acetonitrile (4 mL). White solid 30 mg (14%). mp: 176-178 °C. UPLC-MS (method A): Rt 2.52 min, m/z 418 $[M+H]^+$. ^{1}H NMR (400 MHz, DMSO-d_6) δ . 8.17 – 8.12 (m, 1H), 8.10 (br. s, 1H), 7.89 – 7.77 (m, 3H), 7.72 (d, J = 8.2 Hz, 2H), 7.54 (t, J = 7.7 Hz, 1H), 7.41 (br. s, 1H), 7.21 (d, J = 8.3 Hz, 2H), 7.17 – 7.09 (m, 2H), 7.00 (d, J = 7.8 Hz, 1H), 6.93 (t, J = 7.4 Hz, 1H), 3.18 – 3.05 (m, 2H), 2.91 – 2.76 (m, 4H), 2.61 – 2.51 (m, 4H), 2.44 – 2.29 (m, 2H), 2.23 (s, 3H), 1.61 – 1.43 (m, 4H). ^{13}C NMR (101 MHz, DMSO) δ 167.72, 157.35, 154.21, 151.30, 140.13, 136.21, 134.93, 131.66, 130.75, 129.25, 128.91, 127.87, 127.67 (2C), 126.47, 124.89, 122.70, 122.19 (2C), 118.63, 57.52, 53.23 (2C), 51.37 (2C), 40.41, 28.01, 27.21, 23.62. ESI+ (m/z): $[M+H]^+$ calculated for $C_{29}H_{34}N_4O_3$ 487,2709; found 487,2707 $[M+H]^+$. UPLC-MS Purity (UV @ 215 nm): 95%.

[4-(3-carbamoylphenyl)phenyl] N-[4-[4-[2-(trifluoromethyl)phenyl]piperazin-1-yl] butyl]carbamate (25)

The title compound was synthesized according to the general procedure 3 Method A, starting from di-*tert*-butyldicarbonate (79 mg, 0.36 mmol), 4-dimethylaminopyridine (44 mg, 0.36 mmol) 4-[4-[2-(trifluoromethyl)phenyl]piperazin-1-yl]butan-1-amine (100 mg, 0.33 mmol), and 3-(4-hydroxyphenyl)benzamide (77 mg, 0.36 mmol) in acetonitrile (4 mL). White solid 63 mg (35%). mp: 176-178 °C. UPLC-MS (method A): Rt 2.19 min, m/z 541 $[M+H]^+$. ^{1}H NMR (400

MHz, DMSO-d_6) δ . 8.19 – 8.15 (m, 1H), 8.12 (br. s, 1H), 7.89 – 7.83 (m, 1H), 7.82 – 7.76 (m, 2H), 7.75 – 7.69 (m, 2H), 7.56 – 7.45 (m, 1H), 7.38 (br. s, 1H), 7.34 – 7.27 (m, 2H), 7.25 – 7.19 (m, 2H), 6.92 – 6.86 (m, 2H), 3.18 – 3.05 (m, 2H), 2.89 – 2.81 (m, 4H), 2.50 – 2.42 (m, 4H), 2.35 (t, J = 6.4 Hz, 2H), 1.59 – 1.49 (m, 4H). ^{13}C NMR (101 MHz, DMSO) δ 167.82, 157.49, 154.27, 152.45, 150.96, 140.20, 139.48, 136.25, 134.96, 133.51, 128.93, 128.74, 127.70, 126.87, 125.59, 124.97, 124.33, 122.21 (2C), 115.80 (2C), 57.53, 53.18 (2C), 53.13 (2C), 40.57, 27.24, 23.62. ESI+ (m/z): $[M+H]^+$ calculated for C_{29} H_{31} F_3 N_4 O_3 541,2427; found 541,2423 $[M+H]^+$. UPLC-MS Purity (UV @ 215 nm): 99%.

[4-(3-carbamoylphenyl)phenyl] N-[4-(4-phenylpiperazin-1-yl)butyl]carbamate (26)

The title compound was synthesized according to the general procedure 3 Method B, starting from *p*-nitrophenylchloroformate (42 mg, 0.21 mmol), DIPEA (0.07 mL, 0.42 mmol), 4-(4-phenyl-1-piperidyl)butan-1-amine (45 mg, 0.19 mmol), and 3-(4-hydroxyphenyl)benzamide (45 mg, 0.21 mmol) in a 1:1 mixture of DMA:DCM (4 mL). White solid 14 mg (15%). mp: 91-95 °C. UPLC-MS (method A): Rt 1.92 min, m/z 473 $[M+H]^+$. ^{1}H NMR (400 MHz, DMSO-d_6) δ 8.17 – 8.13 (m, 1H), 8.10 br. s, 1H), 7.88 – 7.78 (m, 2H), 7.75 – 7.69 (m, 2H), 7.54 (t, J = 7.8 Hz, 2H), 7.41 (b. s, 1H), 7.25 – 7.16 (m, 4H), 6.95 – 6.89 (m, 2H), 6.76 (t, J = 7.3 Hz, 1H), 3.17 – 3.06 (m, 6H), 2.51 – 2.43 (m, 4H), 2.37 – 2.30 (m, 2H), 1.59 – 1.48 (m, 4H). ^{13}C NMR (101 MHz, DMSO-d_6) δ 168.96, 157.54, 154.16, 151.80, 140.89, 134.01, 133.02, 129.40, 129.15, 128.85, 128.82, 126.42, 125.87, 120.04, 117.79, 116.30, 56.72, 51.98, 47.69, 40.36, 27.50, 25.56. ESI+ (m/z): $[M+H]^+$ calculated for C_{28} H_{32} N_4 O_3 473,2553; found 473,2556 $[M+H]^+$. UPLC-MS Purity (UV @ 215 nm): 98%.

[4-(3-carbamoylphenyl)-3-fluoro-phenyl] N-[4-[4-(2,3-dichlorophenyl)piperazin-1-yl]butyl]carbamate (27)

The title compound was synthesized according to the general procedure 3 Method A, starting from di-*tert*-butyldicarbonate (73 mg, 0.33 mmol), 4-dimethylaminopyridine (41 mg, 0.33 mmol), 4-[4-(2,3-dichlorophenyl)piperazin-1-yl]butan-1-amine (92 mg, 0.30 mmol), and 3-(2-fluoro-4-hydroxy-phenyl)benzamide (77 mg, 0.33 mmol) in acetonitrile (4 mL). White solid 12 mg (7%). mp: 176-178 °C. UPLC-MS (method A): Rt 2.36 min, m/z 559 $[M+H]^+$. ^{1}H NMR (400 MHz, DMSO-d_6) δ 8.08 (br. s, 1H), 8.04 – 8.01 (m, 1H), 7.98 – 7.86 (m, 2H), 7.68 (d, J = 6.9 Hz, 1H), 7.63 – 7.53 (m, 2H), 7.40 (br. s, 1H), 7.33 – 7.24 (m, 2H), 7.18 (dd, J = 11.7, 2.2 Hz, 1H), 7.15 – 7.05 (m, 2H), 3.16 – 3.06 (m, 2H), 3.03 – 2.94 (m, 4H), 2.63 – 2.51 (m, 4H), 2.40 – 2.32 (m, 2H), 1.59 – 1.46 (m, 4H). ^{13}C NMR (101 MHz, DMSO-d_6) δ 168.96, 160.91 (d, J = 251.8 Hz), 157.54, 154.31 (d, J = 7.7 Hz), 148.43, 133.16, 133.08, 132.47, 130.37 (d, J = 8.6 Hz), 130.02 (d, J = 2.9 Hz), 129.62 (d, J = 2.9 Hz), 129.25, 127.68, 127.01, 126.15, 125.53 (d, J = 20.0 Hz), 125.00, 120.05, 119.56 (d, J = 2.8 Hz), 108.70 (d, J = 20.0 Hz), 56.72, 52.27, 50.49, 40.36, 27.50, 25.56. ESI+ (m/z): $[M+H]^+$ calculated for C_{28} H_{29} Cl_2 F N_4 O_3 559,1679; found 559,1673 $[M+H]^+$. UPLC-MS Purity (UV @ 215 nm): 95%.

[4-(3-carbamoylphenyl)-3-methoxy-phenyl] N-[4-[4-(2,3-dichlorophenyl)piperazin-1-yl]butyl]carbamate (28)

The title compound was synthesized according to the general procedure 3 Method A, starting from di-*tert*-butyldicarbonate (93 mg, 0.43 mmol), 4-dimethylaminopyridine (44 mg, 0.36 mmol) 4-[4-(2,3-dichlorophenyl)piperazin-1-yl]butan-1-amine (80 mg, 0.26 mmol), and 3-(4-hydroxy-2-methoxy-phenyl)benzamide (81 mg, 0.33 mmol) in acetonitrile (4 mL). White solid 35 mg (23%). mp: 176-178 °C. UPLC-MS (method A): Rt 1.91 min, m/z 572 $[M+H]^+$. ^{1}H NMR (400 MHz, DMSO-d_6) δ 7.98 (br s, 1H), 7.96 – 7.91 (m, 1H), 7.86 – 7.78 (m, 2H), 7.61 (d, J = 7.8 Hz, 1H), 7.47 (t, J = 7.7 Hz, 1H), 7.38 – 7.32 (m, 2H), 7.29 (dd, J = 6.9, 3.9 Hz, 2H), 7.14

(dd, *J* = 6.4, 3.1 Hz, 1H), 6.88 (d, *J* = 2.1 Hz, 1H), 6.79 (dd, *J* = 8.3, 2.1 Hz, 1H), 3.75 (s, 3H), 3.16 – 3.08 (m, 2H), 3.04 – 2.94 (m, 4H), 2.60 – 2.52 (m, 4H), 2.42 – 2.34 (m, 2H), 1.60 – 1.48 (m, 4H). ^{13}C NMR (101 MHz, DMSO) δ 167.97, 156.67, 154.16, 151.95, 151.19, 137.66, 134.31, 132.58, 132.00, 130.64, 128.51, 128.33, 127.85, 125.97, 125.91, 125.88, 124.29, 119.52, 114.06, 105.93, 57.38, 55.79, 52.78 (2C), 50.94 (2C), 40.65, 27.23, 23.55. ESI+ (m/z): $[M+H]^+$ calculated for C_{29} H_{32} Cl_2 N_4 O_4 571,1879; found 571,1884 $[M+H]^+$. UPLC-MS Purity (UV @ 215 nm): 98%.

[4-(3-carbamoylphenyl)-3-methoxy-phenyl] N-[4-[4-(2-methoxyphenyl)piperazin-1-yl]butyl]carbamate (29)

The title compound was synthesized according to the general procedure 3 Method A, starting from di-*tert*-butyldicarbonate (93 mg, 0.43 mmol), 4-dimethylaminopyridine (44 mg, 0.36 mmol), 4-[4-(2-methoxyphenyl)piperazin-1-yl]butan-1-amine (80 mg, 0.30 mmol), and 3-(4-hydroxy-2-methoxy-phenyl)benzamide (81 mg, 0.33 mmol) in acetonitrile (4 mL). White solid 35 mg (22%). mp: 176-178 °C. UPLC-MS (method A): Rt 1.88 min, m/z 533 $[M+H]^+$. ^{1}H NMR (400 MHz, DMSO-d_6) δ 8.01 (br. s, 1H), 7.96 – 7.92 (m, 1H), 7.86 (t, *J* = 5.6 Hz, 1H), 7.81 (d, *J* = 7.7 Hz, 1H), 7.61 (d, *J* = 7.8 Hz, 1H), 7.47 (t, *J* = 7.7 Hz, 1H), 7.37 (br. s, 1H), 7.31 (d, *J* = 8.3 Hz, 1H), 6.95 – 6.91 (m, 2H), 6.89 – 6.84 (m, 3H), 6.79 (dd, *J* = 8.3, 2.1 Hz, 1H), 3.76 (s, 3H), 3.75 (s, 3H), 3.17 – 3.05 (m, 2H), 3.03 – 2.88 (m, 4H), 2.58 – 2.49 (m, 4H), 2.40 – 2.29 (m, 2H), 1.59 – 1.46 (m, 4H).^{13}C NMR (101 MHz, DMSO-d_6) δ 168.05, 156.67, 154.28, 152.01, 151.90, 141.31, 137.67, 134.33, 132.14, 130.69, 128.33, 127.97, 126.08, 125.95, 122.40, 120.92, 117.91, 114.05, 111.91, 106.05, 57.65, 55.85, 55.34, 53.09(2C), 50.12 (2C), 40.68, 27.32, 23.66. ESI+ (m/z): $[M+H]^+$ calculated for C_{30} H_{36} N_4 O_5 533,2764; found 533,2767 $[M+H]^+$. UPLC-MS Purity (UV @ 215 nm): 97%.

[4-(3-carbamoylphenyl)phenyl] N-[(E)-4-[4-(2,3-dichlorophenyl)piperazin-1-yl] but-2-enyl]carbamate (30)

The title compound was prepared according to the general procedure 3 Method A starting from di-*tert* butyl carbonate (102 mg, 0.47 mmol), 4-dimethylaminopyridine (49 mg, 0.40 mmol), (E)-4-[4-(2,3-dichlorophenyl)piperazin-1-yl]but-2-en-1-amine (100 mg, 0.33 mmol), and 3-(4-hydroxyphenyl)benzamide (78 mg, 0.37 mmol) in MeCN (3 mL). White solid 28 mg (16%). mp: 176-178 °C. UPLC-MS (method A): Rt 2.36 min, m/z 539 $[M+H]^+$. ^{1}H NMR (400 MHz, DMSO-d_6) δ 8.17 – 8.13 (m, 1H), 8.09 (br. s, 1H), 7.99 (t, J = 5.7 Hz, 1H), 7.85 (d, J = 7.7 Hz, 1H), 7.80 (d, J = 7.9 Hz, 1H), 7.73 (d, J = 8.6 Hz, 2H), 7.54 (t, J = 7.7 Hz, 1H), 7.41 (br. s, 1H), 7.34 – 7.26 (m, 2H), 7.23 (d, J = 8.6 Hz, 2H), 7.14 (dd, J = 6.6, 2.9 Hz, 1H), 5.75 – 5.62 (m, 2H), 3.78 – 3.68 (m, 2H), 3.05 – 2.91 (m, 6H), 2.61 – 2.52 (m, 4H). ^{13}C NMR (101 MHz, DMSO-d_6) δ 168.96, 157.45, 154.16, 148.43, 140.89, 134.01, 133.08, 133.02, 131.95, 129.15, 128.85, 128.82, 128.13, 127.68, 127.01, 126.42, 126.15, 125.87, 120.04, 60.39, 51.71, 50.49, 41.42. ESI+ (m/z): $[M+H]^+$ calculated for C_{28} H_{28} Cl_2 N_4 O_3 539,1617; found 539,1634 $[M+H]^+$. UPLC-MS Purity (UV @ 215 nm): 97%.

[4-(3-carbamoylphenyl)-3-fluoro-phenyl] N-[(E)-4-[4-(2,3-dichlorophenyl) piperazin-1-yl]but-2-enyl]carbamate (31)

The title compound was prepared according to the general procedure 3 Method A starting from di-*tert* butyl carbonate (102 mg, 0.47 mmol), 4-dimethylaminopyridine (49 mg, 0.40 mmol), (E)-4-[4-(2,3-dichlorophenyl)piperazin-1-yl]but-2-en-1-amine (100 mg, 0.33 mmol), and 3-(2-fluoro-4-hydroxy-phenyl)benzamide (85 mg, 0.37 mmol) in MeCN (3 mL). White solid 41 mg (22%). mp: 176-178 °C. UPLC-MS (method A): Rt 2.43 min, m/z 557 $[M+H]^+$. ^{1}H NMR (400 MHz, DMSO-d_6) δ 8.12 – 8.04 (m, 2H), 7.92 – 7.87 (m, 1H), 7.72 – 7.67 (m, 1H), 7.64 –

7.48 (m, 3H), 7.41 (br. s, 1H), 7.32 – 7.26 (m, 2H), 7.21 (dd, *J* = 11.7, 2.3 Hz, 1H), 7.17 – 7.08 (m, 2H), 5.72 – 5.63 (m, 2H), 3.80 – 3.67 (m, 2H), 3.08 – 2.91 (m, 6H), 2.62 – 2.51 (m, 4H). ^{13}C NMR (101 MHz, DMSO-d_6) δ 168.96, 160.91 (d, *J* = 251.8 Hz), 157.45, 154.31 (d, *J* = 7.7 Hz), 148.43, 133.16, 133.08, 132.47, 131.95, 130.37 (d, *J* = 8.6 Hz), 130.02 (d, *J* = 2.9 Hz), 129.62 (d, *J* = 2.9 Hz), 129.25, 128.13, 127.68, 127.01, 126.15, 125.53 (d, *J* = 20.0 Hz), 125.00, 120.05, 119.56 (d, *J* = 2.8 Hz), 108.70 (d, *J* = 20.0 Hz), 60.39, 51.71, 50.49, 41.42. ESI+ (m/z): $[M+H]^+$ calculated for C_{28} H_{27} Cl_2 F N_4 O_3 557,1522; found 557,1517 $[M+H]^+$. UPLC-MS Purity (UV @ 215 nm): 95%.

(4-phenylphenyl) *N*-[3-[4-(2,3-dichlorophenyl)piperazin-1-yl]propyl]carbamate (32)

The title compound was synthesized according to the general procedure 3 Method A, starting from di-*tert*-butyl dicarbonate (85 mg, 0.39 mmol), DMAP (41 mg, 0.33 mmol), 3-[4-(2,3-dichlorophenyl)piperazin-1-yl]propan-1-amine (80 mg, 0.28 mmol), and 4-phenylphenol (52 mg, 0.31 mmol) in CH_3CN (3 mL). White solid 10 mg (7%). mp: 176-178 °C. UPLC-MS (method A): Rt 2.78 min; m/z 484 [M+H]+. ^{1}H NMR (400 MHz, DMSO-d_6) δ 7.80 (t, *J* = 5.7 Hz, 1H), 7.69 – 7.62 (m, 4H), 7.51 – 7.43 (m, 2H), 7.39 – 7.35 (m, 1H), 7.32 – 7.27 (m, 2H), 7.22 – 7.17 (m, 2H), 7.15 (dd, *J* = 6.6, 3.0 Hz, 1H), 3.14 (q, *J* = 6.8 Hz, 2H), 3.05 – 2.92 (m, 4H), 2.62 – 2.54 (m, 4H), 2.42 (t, *J* = 7.0 Hz, 2H), 1.68 (p, *J* = 7.0 Hz, 2H). ^{13}C NMR (101 MHz, DMSO-d_6) δ 154.25, 151.18, 150.66, 140.44, 139.51, 132.65, 130.65, 128.91 (2C), 128.41, 127.49 (2C), 127.29, 126.57 (2C), 124.30, 122.15 (2C), 119.53, 55.15, 52.78 (2C), 50.94 (2C), 39.87, 26.43. ESI+ (m/z): $[M+H]^+$ calculated for C_{27} H_{29} Cl_2 N_3 O_2 498,1715; found 498,1704 $[M+H]^+$. UPLC-MS Purity (UV @ 215 nm): 96%.

(4-phenylphenyl) N-[4-[4-(2,3-dichlorophenyl)piperazin-1-yl]butyl]carbamate (33)

The title compound was synthesized according to the general procedure 3 Method A, starting from di-*tert*-butyldicarbonate (111 mg, 0.51 mmol), 4-dimethylaminopyridine (53 mg, 0.44 mmol) 4-[4-(2,3-dichlorophenyl)piperazin-1-yl]butan-1-amine (110 mg, 0.36 mmol), and 4-phenylphenol (68 mg, 0.40 mmol) in acetonitrile (4 mL). White solid 42 mg (23%). mp: 176-178 °C. UPLC-MS (method A): Rt 3.12 min, m/z 498 $[M+H]^+$. ^{1}H NMR (400 MHz, DMSO-d_6) δ 7.83 (t, J = 5.7 Hz, 1H), 7.68 – 7.61 (m, 4H), 7.50 – 7.43 (m, 2H), 7.38 – 7.33 (m, 1H), 7.31 – 7.26 (m, 2H), 7.21 – 7.16 (m, 2H), 7.13 (dd, J = 6.5, 3.2 Hz, 1H), 3.15 – 3.06 (m, 2H), 3.03 – 2.90 (m, 4H), 2.59 – 2.51 (m, 4H), 2.41 – 2.33 (m, 2H), 1.60 – 1.46 (m, 4H). ^{13}C NMR (101 MHz, DMSO-d_6) δ 154.33, 150.61, 149.52, 139.48, 136.92, 132.72, 128.92 (2C), 128.64, 127.51 (2C), 127.31, 126.58 (2C), 126.04, 125.28, 122.16 (2C), 119.80, 55.06, 51.04 (2C), 47.68 (2C), 40.17, 26.40, 20.49. ESI+ (m/z): $[M+H]^+$ calculated for C_{27} H_{29} Cl_2 N_3 O_2 498,1715; found 498,1704 $[M+H]^+$. UPLC-MS Purity (UV @ 215 nm): 95%.

(4-phenylphenyl) N-[3-[4-(2-methoxyphenyl)piperazin-1-yl]propyl]carbamate hydrochloride (34)

The title compound was synthesized according to the general procedure 3 Method A, starting from di-*tert*-butyldicarbonate (122 mg, 0.56 mmol), 4-dimethylaminopyridine (59 mg, 0.48 mmol), 3-[4-(2-methoxyphenyl)piperazin-1-yl]propan-1-amine (100 mg, 0.40 mmol) and 4-phenylphenol (75 mg, 0.44 mmol) in acetonitrile (4 mL). The resultant oil was dissolved in a small amount of diethyl ether, to which 2M HCl in diethyl ether was added. Evaporation of the solvent produced the title compound as yellow solid 64 mg (33%). mp: 91-95 °C. UPLC-MS (method A): Rt 2.52 min, m/z 446 $[M+H]^+$. ^{1}H NMR (400 MHz, DMSO-d_6) δ 11.22 (br. s, 1H), 7.99 (t, J = 5.8 Hz, 1H), 7.69 – 7.62 (m, 4H), 7.51 – 7.43 (m, 2H), 7.39 – 7.33 (m, 1H), 7.25 – 7.19 (m, 2H), 7.07 – 6.95 (m, 3H), 6.95 – 6.89 (m, 1H), 3.79 (s, 3H), 3.63 – 3.44 (m, 4H), 3.26 –

3.08 (m, 8H), 2.08 – 1.92 (m, 2H). ^{13}C NMR (101 MHz, DMSO-d_6) δ 157.54, 154.16, 150.49, 140.92, 140.50, 133.92, 131.07, 129.17, 128.82, 128.01, 122.36, 120.13, 119.69, 117.71, 114.35, 56.42, 54.54, 52.27, 49.82, 37.82, 24.56. ESI+ (m/z): $[M+H]^+$ calculated for C_{27} H_{31} N_3 O_3 · Cl H 446,2444; found 446,2450 $[M+H]^+$. UPLC-MS Purity (UV @ 215 nm): 98%.

(4-phenylphenyl) N-[4-[4-(2-methoxyphenyl)piperazin-1-yl]butyl]carbamate hydrochloride (35)

The title compound was synthesized according to the general procedure 3 Method A, starting from di-*tert*-butyldicarbonate (116 mg, 0.53 mmol), 4-dimethylaminopyridine (56 mg, 0.46 mmol), 4-[4-(2-methoxyphenyl)piperazin-1-yl]butan-1-amine (100 mg, 0.38 mmol), and 4-phenylphenol (71 mg, 0.42 mmol) in acetonitrile (4 mL). The resultant oil was dissolved in a small amount of diethyl ether, to which 2M HCl in diethyl ether was added. Evaporation of the solvent produced the title compound as yellow solid 54 mg (29%). mp: 91-95 °C. UPLC-MS (method A): Rt 2.54 min, m/z 460 $[M+H]^+$. ^{1}H NMR (400 MHz, DMSO-d_6) δ 11.15 (br. s, 1H), 7.91 (t, J = 5.7 Hz, 1H), 7.70 – 7.61 (m, 4H), 7.49 – 7.42 (m, 2H), 7.40 – 7.33 (m, 1H), 7.24 – 7.17 (m, 2H), 7.06 – 6.88 (m, 4H), 3.79 (s, 3H), 3.59 – 3.39 (m, 4H), 3.27 – 3.06 (m, 8H), 1.89 – 1.74 (m, 2H), 1.53 (p, J = 7.2 Hz, 2H). ^{13}C NMR (101 MHz, DMSO-d_6) δ 154.40, 151.84, 150.66, 139.54, 139.27, 136.98, 129.00 (2C), 127.58 (2C), 127.39, 126.65 (2C), 123.63, 122.27 (2C), 120.88, 118.33, 111.97, 55.42, 55.11, 51.04 (2C), 46.90 (2C), 40.32, 26.48, 20.51. ESI+ (m/z): $[M+H]^+$ calculated for C_{28} H_{33} N_3 O_3 · Cl H 460,26; found 460,2602 $[M+H]^+$. UPLC-MS Purity (UV @ 215 nm): 99%.

(4-phenylphenyl) N-[4-[4-(o-tolyl)piperazin-1-yl]butyl]carbamate (36)

The title compound was synthesized according to the general procedure 3 Method A, starting from di-*tert*-butyldicarbonate (136 mg, 0.62 mmol), 4-dimethylaminopyridine (65 mg, 0.53

mmol), 4-[4-(o-tolyl)piperazin-1-yl]butan-1-amine (110.0 mg, 0.44 mmol), and 4-phenylphenol (83 mg, 0.49 mmol) in acetonitrile (4 mL). White solid 27 mg (14%). mp: 176-178 °C. UPLC-MS (method A): Rt 2.75 min, m/z 444 $[M+H]^+$. ^{1}H NMR (400 MHz, DMSO-d_6) δ .87 (t, J = 5.7 Hz, 1H), 7.68 – 7.63 (m, 4H), 7.46 (t, J = 7.7 Hz, 2H), 7.38 – 7.34 (m, 1H), 7.21 – 7.17 (m, 2H), 7.16 – 7.10 (m, 2H), 7.02 – 6.98 (m, 1H), 6.93 (td, J = 7.4, 1.2 Hz, 1H), 3.15 – 3.06 (m, 2H), 2.86 – 2.78 (m, 4H), 2.59 – 2.49 (m, 4H), 2.42 – 2.33 (m, 2H), 2.23 (s, 3H), 1.57 – 1.49 (m, 4H).^{13}C NMR (101 MHz, DMSO) δ 154.31, 151.33, 150.71, 139.54, 136.88, 131.70, 130.80, 128.96 (2C), 127.54 (2C), 127.33, 126.62 (2C), 126.53, 122.75, 122.21 (2C), 118.67, 57.57, 53.27 (2C), 51.39 (2C), 41.01, 27.26, 23.66, 17.60. ESI+ (m/z): $[M+H]^+$ calculated for C_{28} H_{33} N_3 O_2 444,2651; found 444,2658 $[M+H]^+$. UPLC-MS Purity (UV @ 215 nm): 95%.

(4-phenylphenyl) N-[4-[4-[2-(trifluoromethyl)phenyl]piperazin-1-yl]butyl] carbamate (37)

The title compound was synthesized according to the general procedure 3 Method A, starting from di-*tert*-butyldicarbonate (91 mg, 0.42 mmol), 4-dimethylaminopyridine (44 mg, 0.36 mmol), 4-[4-[2-(trifluoromethyl)phenyl]piperazin-1-yl]butan-1-amine (90 mg, 0.30 mmol), and 4-phenylphenol (56 mg, 0.33 mmol) in acetonitrile (4 mL). White solid 47 mg (32%). mp: 176-178 °C. UPLC-MS (method A): Rt 2.92 min, m/z 498 $[M+H]^+$. ^{1}H NMR (400 MHz, DMSO-d_6) δ 7.91 – 7.84 (m, 1H), 7.68 – 7.59 (m, 6H), 7.57 – 7.50 (m, 1H), 7.49 – 7.42 (m, 2H), 7.39 – 7.28 (m, 2H), 7.23 – 7.16 (m, 2H), 3.15 – 3.06 (m, 2H), 2.91 – 2.80 (m, 4H), 2.58 – 2.43 (m, 4H), 2.40 – 2.29 (m, 2H), 1.56 – 1.45 (m, 4H). ^{13}C NMR (101 MHz, DMSO-d_6) δ 154.30, 152.46, 150.71, 139.54, 136.88, 133.54, 128.94 (2C), 127.53 (2C), 127.31, 126.89, 126.60 (2C), 125.71, 125.43, 125.03, 124.38, 122.18 (2C), 57.52, 53.19 (2C), 53.14 (2C), 40.79, 27.23, 23.61. ESI+ (m/z): $[M+H]^+$ calculated for C_{28} H_{30} F_3 N_3 O_2 498,2368; found 498,2377 $[M+H]^+$. UPLC-MS Purity (UV @ 215 nm): 97%.

9H-carbazol-2-yl N-[3-[4-(2,3-dichlorophenyl)piperazin-1-yl]propyl]carbamate (42)

The title compound was prepared according to the general procedure 3 Method A starting from di-*tert* butyl carbonate (73 mg, 0.33 mmol). 4-dimethylaminopyridine (34 mg, 0.28 mmol), 3-[4-(2,3-dichlorophenyl)piperazin-1-yl]propan-1-amine (80 mg, 0.28 mmol), and 2-hydroxycarbazole (61 mg, 0.33 mmol) in MeCN (3 mL). The title compound (off-white solid) was isolated as free base after chromatographic purification. 14 mg (10%). mp: 176-178 °C. UPLC-MS (method A): Rt 2.88 min, m/z 497 $[M+H]^+$. ^{1}H NMR (400 MHz, DMSO-d_6) δ 11.24 (s, 1H), 8.13 – 8.01 (m, 2H), 7.75 (t, *J* = 5.6 Hz, 1H), 7.47 (d, *J* = 8.0 Hz, 1H), 7.36 (ddd, *J* = 8.1, 7.0, 1.2 Hz, 1H), 7.32 – 7.27 (m, 2H), 7.20 (d, *J* = 2.1 Hz, 1H), 7.18 – 7.11 (m, 2H), 6.88 (dd, *J* = 8.4, 2.1 Hz, 1H), 3.16 (q, *J* = 6.6 Hz, 2H), 3.07 – 2.95 (m, 4H), 2.66 – 2.53 (m, 4H), 2.48 – 2.38 (m, 2H), 1.71 (p, *J* = 7.1 Hz, 2H). ^{13}C NMR (101 MHz, DMSO-d_6) δ 157.54, 152.26, 148.43, 139.00, 138.04, 133.08, 130.70, 127.68, 127.01, 126.15, 123.10, 123.00, 122.43, 120.81, 120.05, 119.56, 117.15, 111.28, 100.85, 54.54, 52.27 (2C), 50.49 (2C), 37.82, 24.56. ESI+ (m/z): $[M+H]^+$ calculated for $C_{26}H_{26}Cl_2N_4O_2$ 497,1511; found 497,1496 $[M+H]^+$. UPLC-MS Purity (UV @ 215 nm): 99%.

9H-carbazol-2-yl N-[4-[4-(2,3-dichlorophenyl)piperazin-1-yl]butyl]carbamate (43)

The title compound was synthesized according to the general procedure 3 Method A, starting from di-*tert*-butyldicarbonate (121 mg, 0.56 mmol), 4-dimethylaminopyridine (58 mg, 0.48 mmol) 4-[4-(2,3-dichlorophenyl)piperazin-1-yl]butan-1-amine (120 mg, 0.40 mmol), and 9H-carbazol-2-ol (80 mg, 0.44 mmol) in acetonitrile (4 mL). White solid 43 mg (21%). mp: 176-178 °C. UPLC-MS (method A): Rt 2.82 min, m/z 512 $[M+H]^+$. ^{1}H NMR (400 MHz, DMSO-d_6) δ 11.25 (br. s, 1H), 8.06 (t, *J* = 8.2 Hz, 2H), 7.78 (t, *J* = 5.6 Hz, 1H), 7.47 (d, *J* = 8.1 Hz, 1H), 7.39 – 7.32 (m, 1H), 7.32 – 7.26 (m, 2H), 7.19 (d, *J* = 2.0 Hz, 1H), 7.18 – 7.11 (m, 2H), 6.87 (dd, *J* =

8.4, 2.1 Hz, 1H), 3.17 – 3.08 (m, 2H), 3.06 – 2.96 (m, 4H), 2.72 – 2.54 (m, 4H), 2.49 – 2.39 (m, 2H), 1.61 – 1.49 (m, 4H). ^{13}C NMR (101 MHz, DMSO-d_6) δ 154.75, 151.09, 149.47, 140.24, 139.98, 132.65, 128.62, 126.03, 125.25, 124.50, 122.24, 120.40, 119.97, 119.62, 118.77, 113.12, 111.13, 104.13, 99.57, 57.24, 52.62 (2C), 50.50 (2C), 40.62, 27.18, 23.23. ESI+ (m/z): $[M+H]^+$ calculated for C_{27} H_{28} Cl_2 N_4 O_2 511,1668; found 511,1674 $[M+H]^+$. UPLC-MS Purity (UV @ 215 nm): 95%.

9H-carbazol-2-yl N-[4-[4-(2-methoxyphenyl)piperazin-1-yl]butyl]carbamate (44)

The title compound was synthesized according to the general procedure 3 Method A, starting from di-*tert*-butyldicarbonate (116 mg, 0.53 mmol), 4-dimethylaminopyridine (56 mg, 0.46 mmol), 4-[4-(2-methoxyphenyl)piperazin-1-yl]butan-1-amine (100 mg, 0.38 mmol), and 9H-carbazol-2-ol (77 mg, 0.42 mmol) in acetonitrile (4 mL). White solid 89 mg (50%). mp: 176-178 °C. UPLC-MS (method A): Rt 2.31 min, m/z 473 $[M+H]^+$. ^{1}H NMR (400 MHz, DMSO-d_6) δ 11.26 (s, 1H), 8.07 (t, *J* = 8.4 Hz, 2H), 7.81 (t, *J* = 5.6 Hz, 1H), 7.47 (d, *J* = 8.1 Hz, 1H), 7.39 – 7.33 (m, 1H), 7.19 (d, *J* = 2.0 Hz, 1H), 7.15 (t, *J* = 7.4 Hz, 1H), 6.96 – 6.82 (m, 5H), 3.76 (s, 3H), 3.18 – 3.06 (m, 2H), 3.04 – 2.88 (m, 4H), 2.57 – 2.50 (m, 4H), 2.40 – 2.31 (m, 2H), 1.61 – 1.45 (m, 4H).^{13}C NMR (101 MHz, DMSO-d_6) δ 154.78, 152.02, 149.51, 141.46, 140.26, 139.94, 125.25, 122.46, 122.20, 120.86, 120.51, 119.93, 119.59, 118.77, 117.90, 113.04, 112.06, 111.14, 104.13, 57.66, 55.37, 53.19 (2C), 50.12 (2C), 40.71, 27.44, 23.67. ESI+ (m/z): $[M+H]^+$ calculated for C_{28} H_{32} N_4 O_3 473,2553; found 473,2561 $[M+H]^+$. UPLC-MS Purity (UV @ 215 nm): 96%.

[3-methoxy-4-phenyl-phenyl] *N*-[4-[4-(2,3-dichlorophenyl)piperazin-1-yl]butyl]carbamate (45)

The title compound was synthesized according to the general procedure 3 Method A, starting from di-*tert*-butyl dicarbonate (202 mg, 0.93 mmol), DMAP (97 mg, 0.79 mmol), 4-[4-(2,3-dichlorophenyl)piperazin-1-yl]butan-1-amine (200 mg, 0.66 mmol), and 3-methoxy-4-phenyl-phenol (172 mg, 0.86 mmol) in CH_3CN (3 mL). White solid 31 mg (9%). mp: 176-178 °C. UPLC-MS (method A): Rt 2.80 min; m/z 528 $[M+H]^+$. ^1H NMR (400 MHz, DMSO-d_6) δ 7.82 (t, J = 5.6 Hz, 1H), 7.47 – 7.43 (m, 2H), 7.40 (t, J = 7.6 Hz, 2H), 7.34 – 7.24 (m, 4H), 7.17 – 7.11 (m, 1H), 6.85 (d, J = 2.1 Hz, 1H), 6.77 (dd, J = 8.2, 2.2 Hz, 1H), 3.74 (s, 3H), 3.16 – 3.07 (m, 2H), 3.04 – 2.94 (m, 4H), 2.60 – 2.52 (m, J = 8.7 Hz, 4H), 2.43 – 2.33 (m, 2H), 1.60 – 1.47 (m, 4H). ^{13}C NMR (101 MHz, DMSO-d_6) δ 156.52, 154.36, 151.25, 137.69, 132.76, 132.58, 132.42, 130.46, 129.18, 128.47, 127.99, 126.75, 126.56, 126.46, 125.93, 124.30, 119.66, 114.02, 105.99, 57.39, 55.72, 52.78 (2C), 50.95 (2C), 40.64, 27.18, 23.63. ESI+ (m/z): $[M+H]^+$ calculated for $C_{28}H_{32}N_4O_3$ 473,2553; found 473,2561 $[M+H]^+$. UPLC-MS Purity (UV @ 215 nm): 99%.

(3-fluoro-4-phenyl-phenyl) *N*-[4-[4-(2,3-dichlorophenyl)piperazin-1-yl]butyl]carbamate (46)

The title compound was synthesized according to the general procedure 3 Method A, starting from di-*tert*-butyl dicarbonate (397 mg, 1.20 mmol), DMAP (97 mg, 1.79 mmol), 4-[4-(2,3-dichlorophenyl)piperazin-1-yl]butan-1-amine (200 mg, 0.66 mmol), and 3-fluoro-4-phenyl-phenol (148 mg, 0.78 mmol) in CH_3CN (3.8 mL). White solid 145 mg (42%). mp: 176-178 °C. UPLC-MS (method A): Rt 2.80 min; m/z 516 [M+H]+. ^1H NMR (400 MHz, DMSO-d_6) δ 7.93 (t, J = 5.6 Hz, 1H), 7.57 – 7.45 (m, 5H), 7.44 – 7.37 (m, 1H), 7.33 – 7.26 (m, 2H), 7.20 – 7.12 (m, 2H), 7.07 (dd, J = 8.5, 2.3 Hz, 1H), 3.11 (q, J = 6.3 Hz, 2H), 3.04 – 2.93 (m, 4H), 2.54 (s, 4H), 2.42 – 2.32 (m, 2H), 1.60 – 1.46 (m, 4H). ^{13}C NMR (101 MHz, DMSO-d_6) δ 159.93, 157.47, 153.76, 151.19, 134.60, 132.58, 130.81, 130.76, 128.71, 128.67, 128.61, 128.40, 127.76,

125.97, 124.29, 119.51, 118.30, 110.21, 109.95, 57.36, 52.77 (2C), 50.94 (2C), 40.94, 27.10, 23.52. ESI+ (m/z): $[M+H]^+$ calculated for C_{28} H_{32} N_4 O_3 473,2553; found 473,2561 $[M+H]^+$. UPLC-MS Purity (UV @ 215 nm): 99%.

(3-methoxy-4-phenyl-phenyl) *N*-[4-[4-(2-methoxyphenyl)piperazin-1-yl]butyl] carbamate (47)

The title compound was synthesized according to the general procedure 3 Method A, starting from di-*tert*-butyldicarbonate (139 mg, 0.64 mmol), 4-dimethylaminopyridine (68 mg, 0.55 mmol), 4-[4-(2-methoxyphenyl)piperazin-1-yl]butan-1-amine (120 mg, 0.46 mmol), and 3-methoxy-4-phenyl-phenol (100 mg, 0.50 mmol) in acetonitrile (4 mL). Yellow solid 94 mg (42%). mp: 200-202 °C. UPLC-MS (method A): Rt 2.52 min, m/z 490 $[M+H]^+$. ^{1}H NMR (400 MHz, DMSO-d_6) δ 7.94 (t, J = 5.7 Hz, 1H), 7.47 – 7.43 (m, 2H), 7.39 (t, J = 7.6 Hz, 2H), 7.34 – 7.28 (m, 1H), 7.25 (d, J = 8.3 Hz, 1H), 7.04 – 6.85 (m, 5H), 6.78 (dd, J = 8.2, 2.1 Hz, 1H), 3.78 (s, 3H), 3.74 (s, 3H), 3.50 – 3.39 (m, 4H), 3.23 – 3.02 (m, 8H), 1.86 – 1.72 (m, 2H), 1.60 – 1.47 (m, 2H). ^{13}C NMR (101 MHz, DMSO-d_6) δ 156.63, 154.28, 152.07, 151.56, 141.28, 137.67, 130.53, 129.24 (2C), 128.06 (2C), 126.82, 126.51, 122.56, 120.68, 117.92, 113.97, 111.90, 106.01, 57.48, 55.76, 55.38, 52.96 (2C), 50.01 (2C), 40.47, 27.23, 23.47. ESI+ (m/z): $[M+H]^+$ calculated for C_{29} H_{35} N_3 O_4 490,2706; found 490,2689 $[M+H]^+$. UPLC-MS Purity (UV @ 215 nm): 99%.

b. Pharmacology

Cell culture conditions. Hek293 cells stably transfected with human FAAH-1 were used as an enzyme source (membrane enrichment) to evaluate FAAH-1 activity. CHO-K1 stably expressing human D2R short were used to perform cell-based cAMP assay to determine D2R activation.

Cells were maintained in DMEM or DMEM:Ham's F-12 1:1, respectively, both supplemented with 10% FBS. 500 μg/mL G418 were added to culture medium to maintain selective pressure. Activities on D3R and CB_1R were assayed on a human D3R and human CB_1R expressing CHO cells.

Human recombinant Fatty Acid Amide Hydrolase (FAAH-1) fluorescent assay. The detailed procedure was recently described in reference 29. Briefly, the assay was run in 96-well microplates (Black OptiPlate-96 F; PerkinElmer, Massachusetts, USA) in a total reaction volume of 180 μL. FAAH-1 membrane-enriched lysate (2,5 μg) was pre-incubated for 50 minutes with various concentrations of test compounds or vehicle control (2,5% DMSO) in assay buffer (50mM Tris-HCl pH7.4, 0.05% Fatty acid-free BSA). Then 1 μM substrate (AMC Arachidonyl Amide; A6855, Sigma) was added and the reaction carried out for 4 hours at 37 °C. Fluorescence was measured with EnVision 2014 Multilabel Reader (PerkinElmer, Massachusetts, USA) using an excitation wavelength of 355 nm and an emission of 460 nm. The results are expressed as a percentage of the total enzymatic activity (protein preparation incubated with the vehicle control).

D3R, D2R-short Dopamine receptors, and CB_1R cellular assay. Activities on D2R-short were tested with an HTRF-cAMP functional assay (cAMP dynamic 2, CISBIO Bioassays). Stably transfected human-DRD2short-expressing CHO-K1 cells were suspended in assay buffer made up of HBSS (Life Technologies) complemented with 20 mM Hepes/NaOH (pH 7.4), 0.1% BSA and 200 μM IBMX. Cells were seeded at a density of 10^4 cells/well in 384 well microplates (384 Well Small Volume HiBase Polystyrene Microplates, Greiner) and pre-incubated for 10 minutes at room temperature (RT) in the presence of either the HBSS (basal control), the reference agonist (stimulated control), or various concentrations of the test compounds. Subsequently, the

adenylyl cyclase activator NKH 477 (N3290, Sigma) was added at a final concentration of 0.5 μM. Following 45 minutes incubation at RT, the fluorescence acceptor (D2-labeled cAMP) and fluorescence donor (anti-cAMP antibody labeled with europium cryptate) were added. After 1 hour at RT, the time-resolved fluorescence was measured at λex=320 nm and λem=620 and 665 nm using EnVision 2014 Multilabel Reader (PerkinElmer, Massachusetts, USA). The cAMP concentration was determined by dividing the signal measured at 665 nm by that measured at 620 nm (ratio). The results are expressed as a percentage of the control response to 300 nM dopamine. D3R and CB-1 assays were run by CEREP (Le Bois l'Evêque, FR), as previously described in reference 28.

Analysis of the Biological Data. Dose-response curves were run in at least two independent experiments, performed in three technical replicates. For compounds assayed on D2R-short and FAAH-1, concentrations were corrected by NMR determinations. EC_{50} or IC_{50} values (concentrations causing half-maximal response or inhibition of control agonist response) were determined by nonlinear regression analysis of the log [concentration]/response curves generated with mean replicate values using a four parameter Hill equation curve fitting with GraphPad Prism 5 (GraphPad Software Inc., CA – USA).

c. PK studies

***In vitro* Plasma Stability Study.** 10 mM DMSO stock solution of test compound was diluted 20-fold with DMSO-H_2O (1:1) and incubated at 37 ˚C for 2 h with *rat* plasma added 5% DMSO (pre-heated at 37 ˚C for 10 min). The final concentration was 2 μM. At each time point (0, 5, 15, 30, 60, 120 min), 50 μL of incubation mixture was diluted with 200 μL cold CH_3CN spiked with 200 nM of internal standard, followed by centrifugation at 3500 g for 20 min. The supernatant was further diluted with H_2O (1:1) for analysis. The concentration of test compound was

quantified by LC/MS-MS. The percentage of test compound remaining at each time point relative to t=0 was calculated. The half-lives ($t_{½}$) were determined by a one-phase decay equation using a nonlinear regression of compound concentration versus time, and were reported as mean values along with their standard deviations (*n = 3*).

The analyses were performed on a Waters ACQUITY UPLC/MS TQD system consisting of a TQD (triple quadrupole detector) Mass Spectrometer equipped with an Electrospray Ionization interface and a Photodiode Array eλ Detector. The analyses were run on an ACQUITY UPLC BEH C_{18} (50x2.1mmID, particle size 1.7µm) with a VanGuard BEH C_{18} pre-column (5x2.1mmID, particle size 1.7µm) at 40 °C, using 0.1% HCOOH in H_2O (A) and 0.1% HCOOH in CH_3CN (B) as mobile phase. Electrospray ionization (ESI) was applied in positive mode. Compound-dependent parameters, such as MRM transitions and collision energy, were developed for each compound.

In Vitro Microsomal Stability Study. 10mM DMSO stock solution of test compound was pre-incubated at 37 ˚C for 15min with rat liver microsomes added 0.1M Tris-HCl buffer (pH 7.4). The final concentration was 4.6 µM. After pre-incubation, the cofactors (NADPH, G6P, G6PDH, and $MgCl_2$ pre-dissolved in 0.1M Tris-HCl) were added to the incubation mixture and the incubation was continued at 37 ˚C for 1h. At each time point (0, 5, 15, 30, 60min), 30 µL of incubation mixture was diluted with 200 µL cold CH_3CN spiked with 200 nM of internal standard, followed by centrifugation at 3500 g for 15min. The supernatant was further diluted with H_2O (1:1) for analysis. The concentration of test compound was quantified by LC/MS-MS. The percentage of test compound remaining at each time point relative to t=0 was calculated. The half-lives ($t_{½}$) were determined by a one-phase decay equation using a non-linear regression

of compound concentration versus time and were reported as mean values along with their standard deviations ($n = 3$).

The analyses were performed on a Waters ACQUITY UPLC/MS TQD system consisting of a TQD (triple quadrupole detector) Mass Spectrometer equipped with an Electrospray Ionization interface and a Photodiode Array eλ Detector. The analyses were run on an ACQUITY UPLC BEH C_{18} (50x2.1mmID, particle size 1.7 μm) with a VanGuard BEH C_{18} pre-column (5x2.1mmID, particle size 1.7 μm) at 40 °C, using 0.1% HCOOH in H_2O (A) and 0.1% HCOOH in CH_3CN (B) as mobile phase. Electrospray ionization (ESI) was applied in positive mode. Compound-dependent parameters, such as MRM transitions and collision energy, were developed for each compound.

Animals. We used male Sprague-Dawley rats, weighing 175–200 g (Charles River, Calco, Italy). Animals were group-housed in ventilated cages and had free access to food and water. They were maintained under a 12-hour light/dark cycle (lights on at 8:00 am) at a controlled temperature (21 ± 1 °C) and relative humidity (55 ± 10%). All experiments were carried out in accordance with the guidelines established by the European Communities Council Directive (Directive 2010/63/EU of 22 September 2010) and approved by the National Council on Animal Care of the Italian Ministry of Health. All efforts were made to minimize animal suffering and to use the minimal number of animals required to produce reliable results.

Pharmacokinetics methods. Compound **33** was administered orally (PO) and intravenously (IV) to cannulated Sprague-Dawley rats at 3 and 10 mg/kg dose. Vehicle was PEG400/Tween 80/Saline solution at 10/10/80% in volume, respectively. Three animals per dose were treated.

Blood samples at 0, 15, 30, 60, 120, 240, 480 and 1440 min after administration were collected for PO arm. Blood samples at 0, 5, 15, 30, 60, 120 and 240 min after administration were collected for IV arm. Plasma was separated from blood by centrifugation for 15 min at 3500 rpm a 4 °C, collected in an Eppendorf tube, and frozen (-80 °C). Control animals treated with vehicle only were also included in the experimental protocol.

Sample preparation brain exposure analysis. Three animals per dose were treated. Compound **33** was dissolved in PEG400/Tween 80/Saline solution at 10/10/80% in volume, respectively, and administered orally at the dose of 10 mg kg−1. After 1 h and 4 h, rats were sacrificed and brains were immediately dissected, frozen on dry ice, and stored at −80 °C until analysis.
Brain samples were homogenized in RIPA buffer (150 mM NaCl, 1.0% Triton X-100, 0.5% sodium deoxycholate, 0.1% sodium dodecyl sulphate, 50 mM Tris, pH 8.0) and were then split in two aliquots kept at -80 °C until analysis. An aliquot was used for compound brain level evaluations. The second aliquot was kept for protein content evaluation by BCA assay.

Pharmacokinetic Study. Samples (plasma and brain homogenate) were thawed in an ice bath, then centrifuged for 20 min. An aliquot of each (50 µL) was transferred into a 96-deepwell plate and added with 150 µL of the extraction solution, consisting of cold acetonitrile spiked with 200 nM of a structural analog of the analyte (compound **32**, closely eluting with the analyte itself) as internal standard. After agitation (3 min) the plate was centrifuged at 3000 g for 20 min at 4°C. 80 µL of supernatant was then transferred into a 96-well plate and added with 80 µL of water. Standard compound was spiked in neat solvent (PBS pH 7.4 added with 20% acetonitrile) to prepare a calibration curve over the 1 nM – 10 µM range. 3 quality control samples were also prepared, spiking the compound in blank mouse plasma to final 20, 200 and 2000 nM concentrations. Calibrators and QCs were crashed with the same extraction solution used for the

plasma samples. Dosing solutions, previously diluted 100000 fold in the neat solvent, were also included in the samples and tested. Plasma and brain levels were monitored on a Waters ACQUITY UPLC/MS TQD system consisting of a TQD (Triple Quadrupole Detector) mass spectrometer equipped with an electrospray ionization interface; 3 uL of each sample were injected on a reversed phase column (Acquity UPLC BEH C18 2.1 X 50 mm, 1.7 µm particle size), and separated with a linear acetonitrile gradient. Column and UPLC-MS system were purchased from Waters Inc. Milford, USA. Flow rate was set to 0.5 mL/min. Eluents were A = water and B = acetonitrile, both added with 0.1% formic acid. After 0.5 min at 10% B, a linear gradient of B was applied from 10% to 100% in 2 min then held at 100% for 10 sec. After the gradient, the system was reconditioned at 10% B for 1 min. Compounds were quantified by monitoring their MRM peak areas: (Compound **33**: m/z = 498 -> 285 at 38 eV of collision energy and m/z = 498 -> 328 at 38 eV of collision energy; Compound **32**-Internal Standard: m/z = 484-> 254at 35 eV of collision energy), and the response factors, calculated on the basis of the internal standard peak area, were then plotted over the calibration curve. MS parameters were: positive ion mode; capillary 2.5 KV; cone 55 V; source temperature 130 °C; cone gas 100L/Hr; desolvation gas 800 L/Hr; desolvation temperature 400 °C. The time/concentration profiles measured with the above-mentioned system were then analyzed using PK Solutions Excel application (Summit Research Service, USA) to derive the pharmacokinetic data (maximum observed concentration (Cmax); maximum time (Tmax); cumulative area under curve (AUC) for experimental time points; distribution volume (Vd); and systemic clearance (Cl)).

d. Computational methods

Three-dimensional alignment of the training set molecules. The starting structural alignment was built based on a rigid template, namely the 3D structure of **33** with the aliphatic side chain perpendicular to the plane of the proximal ring in line with the CB_1R bound conformation of the molecule, which has been consistently hypothesized in previous modeling studies. Compound **4** was structurally aligned to the template by means of the Atomic Property Fields (APF) procedure developed by Totrov and summarized only briefly here.[46] All molecules were assigned MMFF parameters.[53] Seven continuous 3D grid potentials representing the hydrogen bond donor and acceptor propensity, lipophilicity, size, charge, hybridization, and electronegativity of the template were calculated. Molecule **4** was globally optimized within the pre-calculated APF by means of the biased probability Monte Carlo (BPMC) stochastic optimizer implemented in ICM.[54] The intramolecular force-field energy was also considered so as to avoid introducing unrealistic strain into the generated conformations. In turn, compounds **2**-**3**, **16**-**17**, **21**-**24**, **27**, **29**-**33**, and **42**-**44** were individually superimposed according to the same procedure to the generated conformation of **4**.

3D QSAR model. The APF 3D QSAR methodology was adopted in order to create a predictive model for CB_1R activity. For each aligned molecule, the 7-component APF were calculated and pooled together. Each molecule was originally described by its fit, according to the conformation assigned in the alignment, in each of the 126 APF. Based on the activity data at CB_1R, the proper weight for the contributions of each compound to each APF component had to be defined in order to provide quantitative predictions of activity for new compounds. Optimal weights were assigned by the partial least squares (PLS) methodology. The optimal number of latent vectors for PLS was established by leave-one-out cross-validation on the training set. Then, weighted

individual contributions were added together. The new compounds' activities could thus be estimated by simply calculating their fit within the combined QSAR APF.

SUPPORTING INFORMATION.

Syntheses of the intermediates and ^{1}H and ^{13}C-NMR spectra of **33**.

CORRESPONDING AUTHOR

* Giovanni Bottegoni, phone: +3901071781522, e-mail: giovanni.bottegoni@iit.it.

PRESENT ADDRESSES

† Alessio De Simone: School of Chemistry, The University of Edinburgh, David Brewster Road, Edinburgh, EH9 3FJ, UK; Gian Filippo Ruda: Target Discovery Institute - Structural Genomic Consortium, Nuffield Department of Medicine, University of Oxford, Old Road Campus Oxford OX3 7FZ, UK; Alessandra Micoli: Aptuit Srl, Verona, 37135, Italy.

AUTHOR CONTRIBUTIONS

The manuscript was written through contributions of all authors. All authors have given approval to the final version of the manuscript.

ACKNOWLEDGMENT

The authors acknowledge the contribution of Silvia Venzano (compound handling). We thank Grace Fox for copyediting and proofreading the manuscript.

ABBREVIATIONS

D3R, Dopamine Receptor Subtype D_3; *FAAH*, Human Fatty Acid Amide Hydrolase; CB_1R, Cannabinoid Receptor CB_1; MTDL, Multi-Target Directed Ligand.

REFERENCES

(1) Hopkins, A. L. Network pharmacology: the next paradigm in drug discovery. *Nat. Chem. Biol.* **2008,** *4*, 682-690.

(2) Bolognesi, M. L. Polypharmacology in a single drug: multitarget drugs. *Curr. Med. Chem.* **2013,** *20*, 1639-1645.

(3) Peters, J. U. Polypharmacology - foe or friend? *J. Med. Chem.* **2013,** *56*, 8955-8971.

(4) Barabasi, A.-L.; Gulbahce, N.; Loscalzo, J. Network medicine: a network-based approach to human disease. *Nat. Rev. Genet.* **2011,** *12*, 56-68.

(5) Bolognesi, M. L.; Matera, R.; Minarini, A.; Rosini, M.; Melchiorre, C. Alzheimer's disease: new approaches to drug discovery. *Curr. Opin. Chem. Biol.* **2009,** *13*, 303-308.

(6) Prati, F.; Cavalli, A.; Bolognesi, M. L. Navigating the chemical space of multitarget-directed ligands: from hybrids to fragments in alzheimer's disease. *Molecules* **2016,** *21*, 466-478.

(7) Dar, A. C.; Das, T. K.; Shokat, K. M.; Cagan, R. L. Chemical genetic discovery of targets and anti-targets for cancer polypharmacology. *Nature* **2012,** *486*, 80-84.

(8) Knight, Z. A.; Lin, H.; Shokat, K. M. Targeting the cancer kinome through polypharmacology. *Nat. Rev. Cancer* **2010,** *10*, 130-137.

(9) Cavalli, A.; Bolognesi, M. L. Neglected tropical diseases: multi-target-directed ligands in the search for novel lead candidates against Trypanosoma and Leishmania. *J. Med. Chem.* **2009,** *52*, 7339-7359.

(10) Syed, B. A.; Chaudhari, K. Smoking cessation drugs market. *Nat. Rev. Drug Discov.* **2013,** *12*, 97-98.

(11) World Health Organization, *Report on the global tobacco epidemic: enforcing bans on tobacco advertising, promotion and sponsorship*. World Health Organization: Geneva, 2013.

(12) Benowitz, N. L. Pharmacology of nicotine: addiction, smoking-induced disease, and therapeutics. *Annu. Rev. Pharmacol. Toxicol.* **2009,** *49*, 57-71.

(13) D'Souza, M. S.; Markou, A. Neuronal mechanisms underlying development of nicotine dependence: implications for novel smoking-cessation treatments. *Addict. Sci. Clin. Pract.* **2011,** *6*, 4-16.

(14) Picciotto, M. R.; Mineur, Y. S. Molecules and circuits involved in nicotine addiction: The many faces of smoking. *Neuropharmacology* **2014,** *76 Pt B*, 545-553.

(15) Fernandez-Ruiz, J.; Hernandez, M.; Ramos, J. A. Cannabinoid-dopamine interaction in the pathophysiology and treatment of CNS disorders. *CNS Neurosci. Ther.* **2010,** *16*, e72-91.

(16) Melis, M.; Pistis, M.; Perra, S.; Muntoni, A. L.; Pillolla, G.; Gessa, G. L. Endocannabinoids mediate presynaptic inhibition of glutamatergic transmission in rat ventral tegmental area dopamine neurons through activation of CB1 receptors. *J. Neurosci.* **2004,** *24*, 53-62.

(17) Hartmann-Boyce, J.; Stead, L. F.; Cahill, K.; Lancaster, T. Efficacy of interventions to combat tobacco addiction: Cochrane update of 2012 reviews. *Addiction* **2013,** *108*, 1711-1721.

(18) Mihalak, K. B.; Carroll, F. I.; Luetje, C. W. Varenicline is a partial agonist at alpha4beta2 and a full agonist at alpha7 neuronal nicotinic receptors. *Mol. Pharmacol.* **2006,** *70*, 801-805.

(19) Crooks, P. A.; Bardo, M. T.; Dwoskin, L. P. Nicotinic receptor antagonists as treatments for nicotine abuse. *Adv. Pharmacol.* **2014,** *69*, 513-551.

(20) Micheli, F. Recent advances in the development of dopamine D3 receptor antagonists: a medicinal chemistry perspective. *ChemMedChem* **2011,** *6*, 1152-1162.

(21) Newman, A. H.; Blaylock, B. L.; Nader, M. a.; Bergman, J.; Sibley, D. R.; Skolnick, P. Medication discovery for addiction: Translating the dopamine D3 receptor hypothesis. *Biochem. Pharmacol.* **2012,** *84*, 882-890.

(22) Newman, A. H.; Grundt, P.; Nader, M. A. Dopamine D3 receptor partial agonists and antagonists as potential drug abuse therapeutic agents. *J. Med. Chem.* **2005,** *48*, 3663-3679.

(23) Moreira, F. A.; Dalley, J. W. Dopamine receptor partial agonists and addiction. *Eur. J. Pharmacol.* **2015,** *752*, 112-115.

(24) Heidbreder, C. A.; Newman, A. H. Current perspectives on selective dopamine D(3) receptor antagonists as pharmacotherapeutics for addictions and related disorders. *Ann. N.Y. Acad. Sci.* **2010,** *1187*, 4-34.

(25) Keck, T. M.; John, W. S.; Czoty, P. W.; Nader, M. A.; Newman, A. H. Identifying Medication Targets for Psychostimulant Addiction: Unraveling the Dopamine D3 Receptor Hypothesis. *J. Med. Chem.* **2015,** *58*, 5361-5380.

(26) Scherma, M.; Panlilio, L. V.; Fadda, P.; Fattore, L.; Gamaleddin, I.; Le Foll, B.; Justinova, Z.; Mikics, E.; Haller, J.; Medalie, J.; Stroik, J.; Barnes, C.; Yasar, S.; Tanda, G.; Piomelli, D.; Fratta, W.; Goldberg, S. R. Inhibition of anandamide hydrolysis by cyclohexyl carbamic acid 3'-carbamoyl-3-yl ester (URB597) reverses abuse-related behavioral and neurochemical effects of nicotine in rats. *J. Pharmacol. Exp. Ther.* **2008,** *327*, 482-490.

(27) Parsons, L. H.; Hurd, Y. L. Endocannabinoid signalling in reward and addiction. *Nat. Rev. Neurosci.* **2015,** *16*, 579-594.

(28) Panlilio, L. V.; Justinova, Z.; Goldberg, S. R. Inhibition of FAAH and activation of PPAR: new approaches to the treatment of cognitive dysfunction and drug addiction. *Pharmacol. Ther.* **2013,** *138*, 84-102.

(29) Melis, M.; Pillolla, G.; Luchicchi, A.; Muntoni, A. L.; Yasar, S.; Goldberg, S. R.; Pistis, M. Endogenous fatty acid ethanolamides suppress nicotine-induced activation of mesolimbic dopamine neurons through nuclear receptors. *J. Neurosci.* **2008,** *28*, 13985-13994.

(30) Kathuria, S.; Gaetani, S.; Fegley, D.; Valino, F.; Duranti, A.; Tontini, A.; Mor, M.; Tarzia, G.; La Rana, G.; Calignano, A.; Giustino, A.; Tattoli, M.; Palmery, M.; Cuomo, V.; Piomelli, D. Modulation of anxiety through blockade of anandamide hydrolysis. *Nature medicine* **2003,** *9*, 76-81.

(31) De Simone, A.; Ruda, G. F.; Albani, C.; Tarozzo, G.; Bandiera, T.; Piomelli, D.; Cavalli, A.; Bottegoni, G. Applying a multitarget rational drug design strategy: the first set of modulators with potent and balanced activity toward dopamine D3 receptor and fatty acid amide hydrolase. *Chem. Commun. (Camb.)* **2014,** *50*, 4904-4907.

(32) Micoli, A.; De Simone, A.; Russo, D.; Ottonello, G.; Colombano, G.; Ruda, G. F.; Bandiera, T.; Cavalli, A.; Bottegoni, G. Aryl and heteroaryl N-[4-[4-(2,3-substituted-phenyl)piperazine-1-yl]alkyl]carbamates with improved physico-chemical properties as dual modulators of dopamine D3 receptor and fatty acid amide hydrolase. *MedChemComm* **2016,** *7*, 537-541.

(33) Del Zotto, A.; Amoroso, F.; Baratta, W.; Rigo, P. Very Fast Suzuki-Miyaura Reaction Catalyzed by Pd(OAc)2 under Aerobic Conditions at Room Temperature in EGME/H2O. *Eur. J. Org. Chem.* **2008,** *2009*, 110-116.

(34) Moreno-Sanz, G.; Duranti, A.; Melzig, L.; Fiorelli, C.; Ruda, G. F.; Colombano, G.; Mestichelli, P.; Sanchini, S.; Tontini, A.; Mor, M.; Bandiera, T.; Scarpelli, R.; Tarzia, G.; Piomelli, D. Synthesis and structure-activity relationship studies of O-biphenyl-3-yl carbamates

as peripherally restricted fatty acid amide hydrolase inhibitors. *J. Med. Chem.* **2013,** *56*, 5917-5930.

(35) Grundt, P.; Carlson, E. E.; Cao, J.; Bennett, C. J.; McElveen, E.; Taylor, M.; Luedtke, R. R.; Newman, A. H. Novel Heterocyclic Trans Olefin Analogues of N-{4-[4-(2,3-Dichlorophenyl)piperazin-1-yl]butyl}arylcarboxamides as Selective Probes with High Affinity for the Dopamine D3 Receptor. *J. Med. Chem.* **2005,** *48*, 839-848.

(36) Newman, A. H.; Beuming, T.; Banala, A. K.; Donthamsetti, P.; Pongetti, K.; LaBounty, A.; Levy, B.; Cao, J.; Michino, M.; Luedtke, R. R.; Javitch, J. A.; Shi, L. Molecular determinants of selectivity and efficacy at the dopamine D3 receptor. *J. Med. Chem.* **2012,** *55*, 6689-6699.

(37) Tarzia, G.; Duranti, A.; Tontini, A.; Piersanti, G.; Mor, M.; Rivara, S.; Plazzi, P. V.; Park, C.; Kathuria, S.; Piomelli, D. Design, synthesis, and structure-activity relationships of alkylcarbamic acid aryl esters, a new class of fatty acid amide hydrolase inhibitors. *J. Med. Chem.* **2003,** *46*, 2352-2360.

(38) Mor, M.; Rivara, S.; Lodola, A.; Plazzi, P. V.; Tarzia, G.; Duranti, A.; Tontini, A.; Piersanti, G.; Kathuria, S.; Piomelli, D. Cyclohexylcarbamic acid 3'- or 4'-substituted biphenyl-3-yl esters as fatty acid amide hydrolase inhibitors: synthesis, quantitative structure-activity relationships, and molecular modeling studies. *J. Med. Chem.* **2004,** *47*, 4998-5008.

(39) Mor, M.; Lodola, A.; Rivara, S.; Vacondio, F.; Duranti, A.; Tontini, A.; Sanchini, S.; Piersanti, G.; Clapper, J. R.; King, A. R.; Tarzia, G.; Piomelli, D. Synthesis and Quantitative Structure-Activity Relationship of Fatty Acid Amide Hydrolase Inhibitors : Modulation at the N-Portion of Biphenyl-3-yl Alkylcarbamates. *J. Med. Chem.* **2008,** *51*, 3487-3498.

(40) Chien, E. Y.; Liu, W.; Zhao, Q.; Katritch, V.; Han, G. W.; Hanson, M. A.; Shi, L.; Newman, A. H.; Javitch, J. A.; Cherezov, V.; Stevens, R. C. Structure of the human dopamine D3 receptor in complex with a D2/D3 selective antagonist. *Science* **2010,** *330*, 1091-1095.

(41) Cortes, A.; Moreno, E.; Rodriguez-Ruiz, M.; Canela, E. I.; Casado, V. Targeting the dopamine D3 receptor: an overview of drug design strategies. *Expert Opin. Drug Discov.* **2016,** *11*, 641-664.

(42) Razdan, R. K., Structure–Activity Relationships of Classical Cannabinoids. In *The Cannabinoid Receptors*, Reggio, P. H., Ed. Humana Press: New York, 2008; pp 3-19.

(43) Ai, R.; Chang, C. E. Ligand-specific homology modeling of human cannabinoid (CB1) receptor. *J. Mol. Graphics Modell.* **2012,** *38*, 155-164.

(44) Fichera, M.; Cruciani, G.; Bianchi, A.; Musumarra, G. A 3D-QSAR study on the structural requirements for binding to CB(1) and CB(2) cannabinoid receptors. *J. Med. Chem.* **2000,** *43*, 2300-2309.

(45) Hua, T.; Vemuri, K.; Pu, M.; Qu, L.; Han, G. W.; Wu, Y.; Zhao, S.; Shui, W.; Li, S.; Korde, A.; Laprairie, R. B.; Stahl, E. L.; Ho, J. H.; Zvonok, N.; Zhou, H.; Kufareva, I.; Wu, B.; Zhao, Q.; Hanson, M. A.; Bohn, L. M.; Makriyannis, A.; Stevens, R. C.; Liu, Z. J. Crystal Structure of the Human Cannabinoid Receptor CB1. *Cell* **2016,** *167*, 750-762.e714.

(46) Totrov, M. Atomic property fields: generalized 3D pharmacophoric potential for automated ligand superposition, pharmacophore elucidation and 3D QSAR. *Chem. Biol. Drug Des.* **2008,** *71*, 15-27.

(47) Jun, Y.; Xi, C.; Brodbeck, R.; Primus, R.; Braun, J.; Wasley, J. W. F.; Thurkauf, A. NGB 2904 and NGB 2849: Two highly selective dopamine D3 receptor antagonists. *Biorg. Med. Chem. Lett.* **1998,** *8*, 2715-2718.

(48) Cherkasov, A.; Muratov, E. N.; Fourches, D.; Varnek, A.; Baskin, II; Cronin, M.; Dearden, J.; Gramatica, P.; Martin, Y. C.; Todeschini, R.; Consonni, V.; Kuz'min, V. E.; Cramer, R.; Benigni, R.; Yang, C.; Rathman, J.; Terfloth, L.; Gasteiger, J.; Richard, A.; Tropsha, A. QSAR modeling: where have you been? Where are you going to? *J. Med. Chem.* **2014,** *57*, 4977-5010.

(49) Schneider, G.; Baringhaus, K.-H., De Novo Design: From Models to Molecules. In *De novo Molecular Design*, Wiley-VCH Verlag GmbH & Co. KGaA: Weinheim, 2013; pp 1-55.

(50) Blankman, J. L.; Simon, G. M.; Cravatt, B. F. A comprehensive profile of brain enzymes that hydrolyze the endocannabinoid 2-arachidonoylglycerol. *Chemistry & biology* **2007,** *14*, 1347-1356.

(51) Leggio, G. M.; Bucolo, C.; Platania, C. B.; Salomone, S.; Drago, F. Current drug treatments targeting dopamine D3 receptor. *Pharmacol. Ther.* **2016,** *165*, 164-177.

(52) Butini, S.; Nikolic, K.; Kassel, S.; Bruckmann, H.; Filipic, S.; Agbaba, D.; Gemma, S.; Brogi, S.; Brindisi, M.; Campiani, G.; Stark, H. Polypharmacology of dopamine receptor ligands. *Prog. Neurobiol.* **2016,** *142*, 68-103.

(53) Halgren, T. A. Merck molecular force field. I. Basis, form, scope, parameterization, and performance of MMFF94. *J. Comput. Chem.* **1996,** *17*, 490-519.

(54) Abagyan, R.; Raush, E.; Totrov, M. ICM Manual v.3.7. http://www.molsoft.com/man/index.html (accessed October 1, 2016).